

# Derivation of the core mass – halo mass relation of fermionic and bosonic dark matter halos from an effective thermodynamical model

Pierre-Henri Chavanis

*Laboratoire de Physique Théorique, Université de Toulouse, CNRS, UPS, France*

We consider the possibility that dark matter halos are made of quantum particles such as fermions or bosons in the form of Bose-Einstein condensates. In that case, they generically have a “core-halo” structure with a quantum core that depends on the type of particle considered and a halo that is relatively independent of the dark matter particle and that is similar to the NFW profile of cold dark matter. The quantum core is equivalent to a polytrope of index  $n = 3/2$  for fermions,  $n = 2$  for noninteracting bosons, and  $n = 1$  for bosons with a repulsive self-interaction in the Thomas-Fermi limit. We model the halo by an isothermal gas with an effective temperature  $T$ . We then derive the core mass – halo mass relation  $M_c(M_v)$  of dark matter halos from an effective thermodynamical model by extremizing the free energy  $F(M_c)$  with respect to the core mass  $M_c$ . We obtain a general relation, valid for an arbitrary polytropic core, that is equivalent to the “velocity dispersion tracing” relation according to which the velocity dispersion in the core  $v_c^2 \sim GM_c/R_c$  is of the same order as the velocity dispersion in the halo  $v_v^2 \sim GM_v/r_v$ . We provide therefore a justification of this relation from thermodynamical arguments. In the case of fermions, we obtain a relation  $M_c \propto M_v^{1/2}$  that agrees with the relation found numerically by Ruffini *et al.* [Mon. Not. R. Astron. Soc. **451**, 622 (2015)]. In the case of noninteracting bosons, we obtain a relation  $M_c \propto M_v^{1/3}$  that agrees with the relation found numerically by Schive *et al.* [Phys. Rev. Lett **113**, 261302 (2014)]. In the case of bosons with a repulsive self-interaction in the Thomas-Fermi limit, we predict a relation  $M_c \propto M_v^{2/3}$  that still has to be confirmed numerically. We also obtain a general approximate core mass – halo mass relation  $M_c(M_v)$  that is valid for bosons with arbitrary repulsive or attractive self-interaction. For an attractive self-interaction, we determine the maximum halo mass  $(M_v)_{\max}$  that can harbor a stable quantum core (dilute axion “star”). Finally, we argue that the fundamental mass scale of the bosonic dark matter particle is  $m_\Lambda = \hbar\sqrt{\Lambda}/c^2 = 2.08 \times 10^{-33} \text{ eV}/c^2$  and that the fundamental mass scale of the fermionic dark matter particle is  $m_\Lambda^* = (\Lambda\hbar^3/Gc^3)^{1/4} = \sqrt{m_\Lambda M_P} = 5.04 \times 10^{-3} \text{ eV}/c^2$  where  $\Lambda$  is the cosmological constant and  $M_P$  is the Planck mass. Their ratio is  $m_\Lambda^*/m_\Lambda = (c^5/G\hbar\Lambda)^{1/4} = 2.42 \times 10^{30}$ . The actual value of the dark matter particle mass is equal to these mass scales multiplied by a large factor that we obtain from our model.

PACS numbers: 95.30.Sf, 95.35.+d, 98.62.Gq

## I. INTRODUCTION

The nature of dark matter (DM) is still unknown and remains one of the greatest mysteries of modern cosmology. The standard cold dark matter (CDM) model works remarkably well at large (cosmological) scales and is consistent with ever improving measurements of the cosmic microwave background (CMB) from WMAP and Planck missions [1, 2]. However, it encounters serious problems at small (galactic) scales. In particular, it predicts that DM halos should be cuspy [3], with a density diverging as  $r^{-1}$  for  $r \rightarrow 0$ , while observations reveal that they have a flat core density [4]. On the other hand, the CDM model predicts an over-abundance of small-scale structures (subhalos/satellites), much more than what is observed around the Milky Way [5]. These problems are referred to as the “cusp problem” and “missing satellite problem”. The expression “small-scale crisis of CDM” has been coined.

In order to solve these problems, some authors have proposed to take the quantum nature of the DM particle

into account.<sup>1</sup> Indeed, quantum mechanics creates an effective pressure even at zero thermodynamic temperature ( $T_{\text{th}} = 0$ ) that may balance the gravitational attraction at small scales and lead to cores instead of cusps. The DM particle could be a fermion, like a massive neutrino, with a mass  $\sim 170 \text{ eV}/c^2$  (see Appendix D of [14]). It could also be a boson in the form of a Bose-Einstein condensate (BEC), like an ultralight axion, with a mass in the range  $2.19 \times 10^{-22} \text{ eV}/c^2 < m < 1.10 \times 10^{-3} \text{ eV}/c^2$  depending whether the bosons are noninteracting or self-interacting (see Appendix D of [14]).

In these quantum models, DM halos have a “core-halo” structure which results from a process of violent collisionless relaxation [15] and gravitational cooling [16–18]. The core stems from the equilibrium between quantum pressure and gravitational attraction. For fermions, the quantum pressure arises from the Pauli exclusion principle like in the case of white dwarfs and neutron stars. For bosons, the quantum pressure arises from the Heisen-

<sup>1</sup> See our previous papers [6, 7] for an exhaustive list of references (more than 200) on the subject. See also the reviews [8–13].

berg uncertainty principle or from the repulsive self-interaction of the bosons like in the case of boson stars. Quantum mechanics stabilizes the halo against gravitational collapse,<sup>2</sup> leading to a flat core instead of a cusp. The quantum core is equivalent to a polytrope of index  $n = 3/2$  for fermions,  $n = 2$  for noninteracting bosons, and  $n = 1$  for bosons with a repulsive self-interaction in the Thomas-Fermi (TF) limit. It is responsible for the finite density of the DM halos at the center. The core mass-radius relation is  $M_c R_c^3 = 1.49 \times 10^{-3} h^6 / G^3 m^8$  for fermions,  $M_c R_c = 5.25 \hbar^2 / G m^2$  for noninteracting bosons, and  $R_c = \pi(a_s \hbar^2 / G m^3)^{1/2}$  for self-interacting bosons in the TF limit. On the other hand, the halo is relatively independent of quantum effects and is similar to the Navarro-Frenk-White (NFW) profile [3] produced in CDM simulations or to the empirical Burkert profile [4] deduced from the observations. It is responsible for the flat rotation curves of the galaxies at large distances. We shall approximate this halo by an isothermal atmosphere with an effective temperature  $T$ .<sup>3</sup> In that case, the density decreases at large distance as  $\rho \propto r^{-2}$  [29], instead of  $r^{-3}$  for the NFW and Burkert profiles, leading exactly to flat rotation curves for  $r \rightarrow +\infty$ . For sufficiently large halos, the halo mass-radius relation is  $M_h = 1.76 \Sigma_0 r_h^2$  [7] where

$$\Sigma_0 = \rho_0 r_h = 141 M_\odot / \text{pc}^2 \quad (1)$$

is the universal surface density of DM halos deduced from the observations [30–32]. Ultracompact halos like dSphs ( $r_h \sim 1 \text{ kpc}$  and  $M_h \sim 10^8 M_\odot$ ) are dominated by the quantum core and have almost no atmosphere. Large halos like the Medium Spiral ( $r_h \sim 10 \text{ kpc}$  and  $M_h \sim 10^{11} M_\odot$ ) are dominated by the isothermal atmosphere.

In a recent paper [7], we have developed of model of DM halos made of bosons with a repulsive self-interaction

in the TF limit. We have obtained a generic phase diagram (see Fig. 49 of [7]) determining the structure of the DM halos (measured by the core mass  $M_c$ ) as a function of their mass  $M_h$ . There is a minimum halo mass  $(M_h)_{\min}$  corresponding to the ground state of the boson gas ( $T = 0$ ) at which the DM halo is a purely quantum object without isothermal halo ( $M_c \simeq M_h$ ). Larger halos have a “core-halo” structure with a quantum core and an isothermal atmosphere. We found a branch along which the core mass  $M_c$  decreases as the halo mass  $M_h$  increases. Rapidly, the core mass becomes negligible and the halos behave as purely isothermal halos without quantum core. However, we found a critical point  $(M_h)_{\text{CCP}}$ , that we interpreted as a canonical critical point, at which a bifurcation occurs. On the new branch, the core mass  $M_c$  increases as the halo mass  $M_h$  increases. On that branch, we found another critical point at a higher mass  $(M_h)_{\text{MCP}}$ , that we interpreted as a microcanonical critical point, above which the quantum core becomes unstable and is replaced by a supermassive black hole resulting from a gravothermal catastrophe followed by a dynamical instability of general relativistic origin. Considering the bifurcated branch with the “core-halo” structure, we developed an effective thermodynamical model to analytically predict the core mass – halo mass relation  $M_c(M_h)$ .<sup>4</sup> We showed that this relation is equivalent to the “velocity dispersion tracing” relation according to which the velocity dispersion in the core  $v_c^2 \sim G M_c / R_c$  is of the same order as the velocity dispersion in the halo  $v_v^2 \sim G M_v / r_v$  [7, 34]. We could provide therefore a justification of this relation from thermodynamical arguments.

In the present paper, we extend this thermodynamical model to the case of DM halos made of fermions and to the case of DM halos made of noninteracting bosons. To unify the formalism, we model the quantum core as a polytrope of arbitrary index  $n$  (with  $n = 3/2$  for fermions,  $n = 2$  for noninteracting bosons, and  $n = 1$  for self-interacting bosons in the TF limit) and we model the atmosphere as an isothermal gas with a uniform density confined within a “box” of radius  $R$ . The radius of the box is identified with the halo radius  $r_h$  and the total mass of the system contained within the box (core + halo) is identified with the halo mass  $M_h$ . They are related by  $M_h = 1.76 \Sigma_0 r_h^2$  [7]. We analytically compute the free energy  $F(M_c)$  of the system. By extremizing  $F(M_c)$  as a function of  $M_c$  for a given value of  $M$  and  $R$  we obtain the core mass  $M_c$  as a function of the halo mass  $M_h$ . We find this relation to be always (for any value of  $n$ ) equivalent to the velocity dispersion tracing relation, thereby generalizing our previous result [7]. We also obtain a general approximate relation  $M_c(M_v)$  that is valid for bosons with arbitrary repulsive or attractive

<sup>2</sup> This is true for the nonrelativistic systems that we consider here. For general relativistic systems, there is a maximum mass  $M_{\text{max}}^{\text{GR}}$  [19–24] above which the system collapses towards a black hole. In our case, we will find that  $M_c \ll M_{\text{max}}^{\text{GR}}$  so that a Newtonian approach is sufficient. On the other hand, if the bosons have an attractive self-interaction, like in the case of the axion [11], there exists a maximum mass  $M_{\text{max}}$  [6] for the quantum core even in the Newtonian regime. Above that limit, the quantum core (dilute axion star) undergoes gravitational collapse.

<sup>3</sup> We approximate the atmosphere by an isothermal sphere but we stress that the temperature is effective and does not correspond to the true thermodynamic temperature (which is almost equal to zero). In particular, the atmosphere does not correspond to a statistical equilibrium state resulting from a “collisional” evolution of the quantum particles of mass  $m$  which would be much too long (much larger than the age of the Universe) [7]. It may rather correspond to an out-of-equilibrium thermodynamical state - or quasistationary state - resulting from a collisionless evolution (independent of  $m$ ) like in Lynden-Bell’s theory of violent relaxation [15]. In the case of fuzzy DM, the approximately isothermal atmosphere (due to quantum interferences of excited states) may also result from the “collisional” evolution of quasi-particles (granules) of the size of the solitonic core and of mass  $m_* \gg m$  as argued in [25–28].

<sup>4</sup> This thermodynamical model was originally introduced in [33] to analytically obtain the caloric curve of self-gravitating fermions.

self-interaction. For an attractive self-interaction, we determine the maximum halo mass  $(M_v)_{\max}$  that can harbor a stable quantum core (dilute axion star). Finally, we use our results to predict the fundamental mass scale of the bosonic or fermionic DM particle in terms of fundamental constants.

The paper is organized as follows. In Sec. II we consider models of DM halos with a quantum (fermionic or bosonic) core and an isothermal atmosphere. In Sec. III we show that these models can be obtained in a unified manner from a generalized wave equation. In Sec. IV we obtain the core mass – halo mass relation of DM halos from an analytical thermodynamical model. This relation is valid for a general polytropic core. In Sec. V we show that this relation is equivalent to the velocity dispersion tracing relation. In Secs. VI and VII we specifically apply these results to DM halos made of fermions, noninteracting bosons and self-interacting bosons.

## II. QUANTUM MODELS OF DM HALOS

In this section, we review quantum models of DM halos made of fermions or bosons. If DM halos are quantum objects, there must be a minimum halo radius  $R$  and a minimum halo mass  $M$  in the Universe corresponding to the ground state ( $T = 0$ ) of the self-gravitating quantum gas. This result is in agreement with the observations. Indeed, there are apparently no DM halos with a radius smaller than  $R \sim 1$  kpc and a mass smaller than  $M \sim 10^8 M_\odot$ , the typical values of the radius and mass of dSphs like Fornax. This observational result cannot be explained by the CDM model which predicts the existence of DM halos at all scales.

Ultracompact dwarf DM halos just have a quantum core without atmosphere (ground state). Larger DM halos have a core-halo structure with a quantum core corresponding to the ground state ( $T = 0$ ) of the quantum gas and an “atmosphere” resulting from violent relaxation and gravitational cooling. The atmosphere has a density profile that can be fitted by the empirical Burkert profile or by NFW profile. In this paper, we shall approximate this density profile by an isothermal profile of effective temperature  $T$ . It is the atmosphere that fixes the size of large halos and explains why their radius increases with their mass as  $M_h \propto r_h^2$  (since  $\Sigma_0$  is constant). By contrast, the radius  $R_c$  of the quantum core usually decreases or remains constant as its mass  $M_c$  increases (see below).

To determine the parameters of the DM particle, we proceed as follows (see Appendix D of [14]).<sup>5</sup> We assume that the smallest halo that has been observed, with a

typical radius and a typical mass

$$R \sim 1 \text{ kpc}, \quad M \sim 10^8 M_\odot, \quad (\text{Fornax}), \quad (2)$$

corresponds to the ground state of a self-gravitating quantum gas. Using the mass-radius relation  $M(R)$  of the self-gravitating quantum gas at  $T = 0$ , we can obtain the parameters of the DM particle. We can then check that the nonrelativistic treatment used in this paper is valid by showing that  $M_c \ll M_{\max}$ .

### A. Fermionic DM

The equation of state of a nonrelativistic Fermi gas at  $T = 0$  is [35]

$$P = \frac{1}{20} \left( \frac{3}{\pi} \right)^{2/3} \frac{h^2}{m^{8/3}} \rho^{5/3}. \quad (3)$$

This is a polytropic equation of state of index  $\gamma = 5/3$  (i.e.  $n = 3/2$ ) and polytropic constant

$$K = \frac{1}{20} \left( \frac{3}{\pi} \right)^{2/3} \frac{h^2}{m^{8/3}}. \quad (4)$$

In the TF approximation, which amounts to neglecting the quantum potential, the fundamental differential equation of hydrostatic equilibrium determining the density profile of a nonrelativistic fermion star<sup>6</sup> at  $T = 0$  with the equation of state (3) writes (see Appendix A)

$$\frac{1}{8} \left( \frac{3}{\pi} \right)^{2/3} \frac{h^2}{m^{8/3}} \Delta \rho^{2/3} = -4\pi G \rho. \quad (5)$$

It can be reduced to the Lane-Emden equation (A8) of index  $n = 3/2$ . This profile has a compact support and the fermion star is stable. The mass-radius relation is

$$M_c R_c^3 = \frac{9\omega_{3/2}}{8192\pi^4} \frac{h^6}{G^3 m^8}, \quad (6)$$

where  $\omega_{3/2} = 132.3843$ . On the other hand, from Eqs. (B7) and (B9) which reduce to<sup>7</sup>

$$E_c = U_c + W_c, \quad (7)$$

$$2U_c + W_c = 0, \quad (8)$$

and from the Betti-Ritter formula (C5), we obtain

$$E_c = -U_c = \frac{1}{2} W_c = -\frac{3}{7} \frac{GM_c^2}{R_c}. \quad (9)$$

<sup>5</sup> Our aim here is not to make an accurate model of DM halos. Therefore, an order of magnitude of the DM particle parameters is sufficient.

<sup>6</sup> In this paper, the name “fermion star” refers to ultracompact DM halos made of fermions or to the fermionic core of larger DM halos (the same comment applies to the names “boson stars”, “BEC stars” and “axion stars” used below).

<sup>7</sup> In the main text, we denote by  $E_c$ ,  $U_c$  and  $W_c$  what are called  $E_{\text{tot}}$ ,  $U$  and  $W$  in the Appendices.

Combined with Eq. (6), we find that the energy of a nonrelativistic fermion star at  $T = 0$  (ground state) is

$$E_c = -\frac{3}{7} \left( \frac{8192\pi^4}{9\omega_{3/2}} \right)^{1/3} \frac{G^2 m^{8/3} M_c^{7/3}}{h^2}. \quad (10)$$

Let us assume that the smallest DM halo that we know, with mass  $M$  and radius  $R$ , corresponds to the ground state of a nonrelativistic self-gravitating Fermi gas. From the mass-radius relation (6), we get

$$\frac{m}{\text{eV}/c^2} = 2.27 \times 10^4 \left( \frac{\text{pc}}{R} \right)^{3/8} \left( \frac{M_\odot}{M} \right)^{1/8}. \quad (11)$$

Using the reference values of  $M$  and  $R$  corresponding to Fornax [see Eq. (2)], we find a fermion mass (see Appendix D of [14]):

$$m = 170 \text{ eV}/c^2. \quad (12)$$

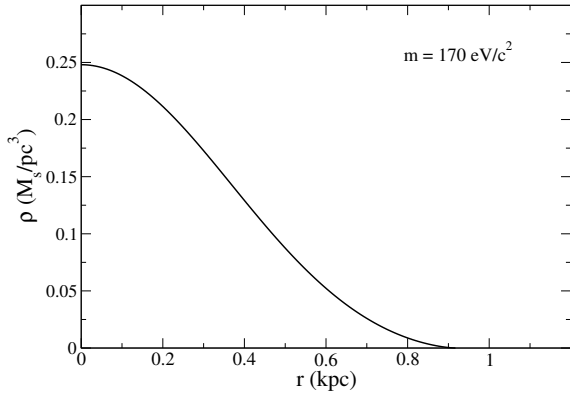


FIG. 1: Density profile of the “minimum halo” (ground state) of surface density  $\Sigma_0 = \rho_0 r_h = 141 M_\odot/\text{pc}^2$  made of fermions of mass  $m = 170 \text{ eV}/c^2$ .

Alternatively, using the results of Appendix G and taking  $m = 170 \text{ eV}/c^2$  in the numerical applications, we find that the minimum halo radius, the minimum halo mass and the maximum central density are

$$(r_h)_{\min} = 1.50 \left( \frac{\hbar^6}{G^3 m^8 \Sigma_0} \right)^{1/5} = 570 \text{ pc}, \quad (13)$$

$$(M_h)_{\min} = 4.47 \left( \frac{\hbar^{12} \Sigma_0^3}{G^6 m^{16}} \right)^{1/5} = 9.09 \times 10^7 M_\odot. \quad (14)$$

$$(\rho_0)_{\max} = 0.667 \left( \frac{\Sigma_0 m^{4/3} G^{1/2}}{\hbar} \right)^{6/5} = 0.248 M_\odot/\text{pc}^3, \quad (15)$$

where  $\Sigma_0$  is the universal density of DM halos given by Eq. (1). These values can be improved if we have a more reliable expression of the fermion mass  $m$ , but they are

sufficient for our purposes (the same comment applies to the bosonic models considered below).

The maximum mass of a fermion star at  $T = 0$  set by general relativity is  $M_{\max} = 0.384 (\hbar c/G)^{3/2}/m^2$  and its minimum radius is  $R_{\min} = 8.73 GM_{\max}/c^2$  [19]. They can be written as

$$\frac{M_{\max}}{M_\odot} = 6.26 \times 10^{17} \left( \frac{\text{eV}/c^2}{m} \right)^2, \quad \frac{R_{\min}}{\text{km}} = 12.9 \frac{M_{\max}}{M_\odot}. \quad (16)$$

For a fermion of mass  $m = 170 \text{ eV}/c^2$ , we obtain  $M_{\max} = 2.17 \times 10^{13} M_\odot$  and  $R_{\min} = 8.85 \text{ pc}$ . The maximum mass is much larger than the typical core mass of a DM halo. Assuming that a fermion star at  $T = 0$  describes the quantum core of a DM halo, we conclude that such cores are nonrelativistic since  $M_c \ll M_{\max}$  in general. Since the maximum mass is much larger than the core mass, gravity can be treated within a Newtonian framework.

## B. Noninteracting bosonic DM

We consider a gas of noninteracting bosons at  $T = 0$  forming a BEC. The wavefunction of a self-gravitating BEC without self-interaction is governed by the Schrödinger-Poisson equation [6]. Using Madelung’s hydrodynamic representation of the Schrödinger equation [36], we find that the fundamental differential equation of quantum hydrostatic equilibrium determining the density profile of the BEC is [6]

$$\frac{\hbar^2}{2m^2} \Delta \left( \frac{\Delta \sqrt{\rho}}{\sqrt{\rho}} \right) = 4\pi G \rho. \quad (17)$$

This equation can be solved numerically [17, 18, 21, 25–27, 37–39]. The density profile of a noninteracting BEC star at  $T = 0$  (ground state) extends to infinity and the BEC star is stable. The mass-radius relation is

$$M_c(R_c)_{99} = 9.95 \frac{\hbar^2}{G m^2}, \quad (18)$$

where  $(R_c)_{99}$  is the radius enclosing 99% of the mass. From Eqs. (B7) and (B9) which reduce to

$$E_c = \Theta_Q^c + W_c, \quad (19)$$

$$2\Theta_Q^c + W_c = 0, \quad (20)$$

we obtain

$$E_c = -\Theta_Q^c = \frac{1}{2} W_c. \quad (21)$$

From numerical computations [21, 37, 38], we find that the total energy of a noninteracting BEC star at  $T = 0$  (ground state) is

$$E_c = -0.0543 \frac{G^2 M_c^3 m^2}{\hbar^2}. \quad (22)$$

Actually, we find in Appendix E that there exists another solution of Eq. (17). It has a compact support and its profile corresponds to a polytrope of index  $\gamma = 3/2$  (i.e.  $n = 2$ ). Its energy is smaller than the energy of the solution considered here, suggesting that it is more stable, even if comparing the energies of stable states may not be decisive in view of the very long lifetime of metastable states in systems with long-range interactions. In the following, in order to develop a unified description of fermions and bosons based on polytropic equations of state, we will use the solution from Appendix E. However, as far as scalings and orders of magnitude are concerned, we would get similar results by using the more conventional (but maybe less stable) solution of this section.

Let us assume that the smallest DM halo that we know, with mass  $M$  and radius  $R$ , corresponds to the ground state of a noninteracting BEC star. From the mass-radius relation (18), we get

$$\frac{m}{\text{eV}/c^2} = 9.22 \times 10^{-17} \left(\frac{\text{pc}}{R}\right)^{1/2} \left(\frac{M_\odot}{M}\right)^{1/2}. \quad (23)$$

Using the reference values of  $M$  and  $R$  corresponding to Fornax [see Eq. (2)], we find a boson mass (see Appendix D of [14]):

$$m = 2.92 \times 10^{-22} \text{ eV}/c^2. \quad (24)$$

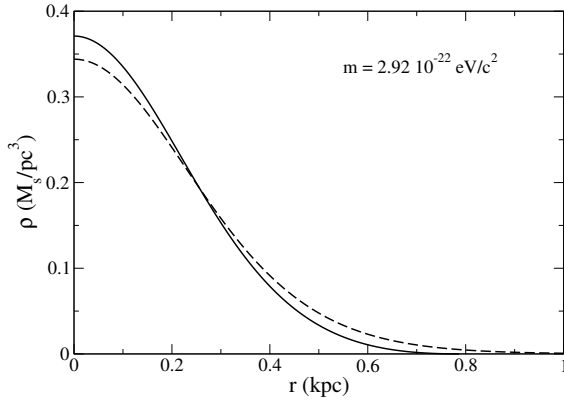


FIG. 2: Density profile of the “minimum halo” (ground state) of surface density  $\Sigma_0 = \rho_0 r_h = 141 M_\odot/\text{pc}^2$  made of non-interacting bosons of mass  $m = 2.92 \times 10^{-22} \text{ eV}/c^2$ . We have plotted the polytropic profile with a compact support obtained in Appendix E (solid line) and the more conventional profile computed in [17, 18, 21, 25–27, 37–39] for which  $(r_h)_{\min} = 410 \text{ pc}$ ,  $(M_h)_{\min} = 4.52 \times 10^7 M_\odot$  and  $(\rho_0)_{\max} = 0.344 M_\odot/\text{pc}^3$  (dashed line taken from [7, 38]).

Alternatively, using the results of Appendix G and taking  $m = 2.92 \times 10^{-22} \text{ eV}/c^2$  in the numerical applications, we find that the minimum halo radius, the minimum halo mass and the maximum central density are (computed

from the polytropic solution)

$$(r_h)_{\min} = 0.913 \left(\frac{\hbar^2}{Gm^2\Sigma_0}\right)^{1/3} = 378 \text{ pc}, \quad (25)$$

$$(M_h)_{\min} = 1.61 \left(\frac{\hbar^4\Sigma_0}{G^2m^4}\right)^{1/3} = 3.89 \times 10^7 M_\odot. \quad (26)$$

$$(\rho_0)_{\max} = 1.09 \frac{G^{1/3}m^{2/3}\Sigma_0^{4/3}}{\hbar^{2/3}} = 0.371 M_\odot/\text{pc}^3, \quad (27)$$

where  $\Sigma_0$  is the universal density of DM halos given by Eq. (1).

The maximum mass of a noninteracting boson star at  $T = 0$  set by general relativity is  $M_{\max} = 0.633 \hbar c/Gm$  and its minimum radius is  $R_{\min} = 9.53 GM_{\max}/c^2$  [20, 21]. They can be written as

$$\frac{M_{\max}}{M_\odot} = 8.48 \times 10^{-11} \frac{\text{eV}/c^2}{m}, \quad \frac{R_{\min}}{\text{km}} = 14.1 \frac{M_{\max}}{M_\odot}. \quad (28)$$

For a boson of mass  $m = 2.92 \times 10^{-22} \text{ eV}/c^2$ , we obtain  $M_{\max} = 2.90 \times 10^{11} M_\odot$  and  $R_{\min} = 0.133 \text{ pc}$ . The maximum mass is much larger than the typical core mass of a DM halo. Assuming that a BEC star at  $T = 0$  (soliton) describes the quantum core of a DM halo, we conclude that such cores are nonrelativistic since  $M_c \ll M_{\max}$  in general. Since the maximum mass is much larger than the core mass, gravity can be treated within a Newtonian framework.

### C. Bosonic DM with a repulsive self-interaction in the TF limit

We consider a gas of self-interacting bosons at  $T = 0$  forming a BEC. The wavefunction of a self-gravitating BEC with a quartic self-interaction is governed by the GPP equations [6]. The equation of state of a self-interacting BEC is [6]

$$P = \frac{2\pi a_s \hbar^2}{m^3} \rho^2, \quad (29)$$

where  $a_s$  is the scattering length of the bosons. This is a polytropic equation of state of index  $\gamma = 2$  (i.e.  $n = 1$ ) and polytropic constant

$$K = \frac{2\pi a_s \hbar^2}{m^3}. \quad (30)$$

We assume that the self-interaction is repulsive ( $a_s > 0$ ). Using Madelung’s hydrodynamic representation of the GPP equations, and taking the quantum potential into account, we find that the fundamental differential equation of quantum hydrostatic equilibrium determining the density profile of the BEC is [6]

$$-\frac{\hbar^2}{2m^2} \Delta \left( \frac{\Delta \sqrt{\rho}}{\sqrt{\rho}} \right) + \frac{4\pi a_s \hbar^2}{m^3} \Delta \rho = -4\pi G \rho. \quad (31)$$

This equation can be solved numerically [38]. The density profile of a noninteracting BEC star at  $T = 0$  (ground state) extends to infinity. The mass-radius relation has been obtained in [6, 38].

In the TF approximation, which amounts to neglecting the quantum potential, the fundamental differential equation of hydrostatic equilibrium determining the density profile of a self-interacting BEC star at  $T = 0$  with the equation of state (29) writes (see Appendix A)

$$\frac{4\pi a_s \hbar^2}{m^3} \Delta \rho = -4\pi G \rho. \quad (32)$$

It can be reduced to the Lane-Emden equation (A8) of index  $n = 1$  which has a simple analytical solution [35]. This profile has a compact support and the self-interacting BEC star is stable. A self-gravitating BEC with a repulsive self-interaction in the TF approximation has a unique radius [6, 23, 40–44],

$$R_c = \pi \left( \frac{a_s \hbar^2}{G m^3} \right)^{1/2}, \quad (33)$$

that is independent of its mass. From Eqs. (B7) and (B9) which reduce to

$$E_c = U_c + W_c, \quad (34)$$

$$3U_c + W_c = 0, \quad (35)$$

and from the Betti-Ritter formula (C5), we obtain

$$E_c = -2U_c = \frac{2}{3} W_c = -\frac{1}{2} \frac{G M_c^2}{R_c}. \quad (36)$$

Combined with Eq. (33), we find that the energy of a self-interacting BEC star at  $T = 0$  (ground state) in the TF limit is

$$E_c = -\frac{1}{2\pi} \frac{G^{3/2} m^{3/2} M_c^2}{a_s^{1/2} \hbar}. \quad (37)$$

Let us assume that the smallest DM halo that we know, with mass  $M$  and radius  $R$ , corresponds to the ground state of a self-interacting BEC star. From Eq. (33), we get

$$\frac{a_s}{\text{fm}} \left( \frac{\text{eV}/c^2}{m} \right)^3 = 3.28 \times 10^{-3} \left( \frac{R}{\text{pc}} \right)^2. \quad (38)$$

This formula depends only on  $R$ . Using the reference values of  $R$  corresponding to Fornax [see Eq. (2)], we find that the ratio  $a_s/m^3$  of the boson parameters  $a_s$  and  $m$  is given by (see Appendix D of [14]):

$$\frac{a_s}{\text{fm}} \left( \frac{\text{eV}/c^2}{m} \right)^3 = 3.28 \times 10^3. \quad (39)$$

In order to determine the mass of the boson, we need another relation. This relation is provided by the constraint  $\sigma/m < 1.25 \text{ cm}^2/\text{g}$  set by the Bullet Cluster [45],

where  $\sigma = 4\pi a_s^2$  is the self-interaction cross section. In Appendix D of [14] we have considered two extreme cases corresponding to an upper boson mass

$$m = 1.10 \times 10^{-3} \text{ eV}/c^2, \quad a_s = 4.41 \times 10^{-6} \text{ fm}, \quad (40)$$

and a lower boson mass

$$m = 2.92 \times 10^{-22} \text{ eV}/c^2, \quad a_s = 8.13 \times 10^{-62} \text{ fm}. \quad (41)$$

We note that when a self-interaction between the bosons is allowed, a large mass window is open. In particular, a repulsive self-interaction allows one to have a larger boson mass than in the noninteracting case. As discussed in Appendix D.4 of [14] this may be interesting in view of the fact that the mass of a noninteracting boson ( $m \sim 1 - 10 \times 10^{-22} \text{ eV}/c^2$ ) is in tension with observations of the Lyman- $\alpha$  forest [27]. This tension could reflect the fact that bosons have a repulsive self-interaction.

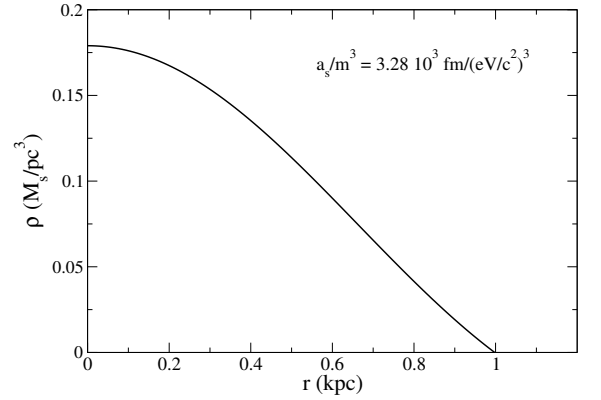


FIG. 3: Density profile of the “minimum halo” (ground state) of surface density  $\Sigma_0 = \rho_0 r_h = 141 M_\odot/\text{pc}^2$  made of self-interacting bosons in the TF limit with  $a_s/m^3 = 3.28 \times 10^3 \text{ fm (eV}/c^2)^{-3}$ .

Alternatively, using the results of Appendix G and taking  $a_s/m^3 = 3.28 \times 10^3 \text{ fm (eV}/c^2)^{-3}$  in the numerical applications, we find that the minimum halo radius, the minimum halo mass and the maximum central density are

$$(r_h)_{\min} = 2.47 \left( \frac{a_s \hbar^2}{G m^3} \right)^{1/2} = 786 \text{ pc}, \quad (42)$$

$$(M_h)_{\min} = 13.0 \frac{a_s \hbar^2 \Sigma_0}{G m^3} = 1.86 \times 10^8 M_\odot. \quad (43)$$

$$(\rho_0)_{\max} = 0.404 \left( \frac{G m^3 \Sigma_0^2}{a_s \hbar^2} \right)^{1/2} = 0.179 M_\odot/\text{pc}^3, \quad (44)$$

where  $\Sigma_0$  is the universal density of DM halos given by Eq. (1).

The maximum mass of a self-interacting boson star set by general relativity is  $M_{\max} = 0.307 \hbar c^2 \sqrt{a_s} / (Gm)^{3/2}$  and its minimum radius is  $R_{\min} = 6.25 G M_{\max} / c^2$  [22–24]. They can be written as

$$\frac{M_{\max}}{M_{\odot}} = 1.12 \left( \frac{a_s}{\text{fm}} \right)^{1/2} \left( \frac{\text{GeV}/c^2}{m} \right)^{3/2}, \quad (45)$$

$$\frac{R_{\min}}{\text{km}} = 9.27 \frac{M_{\max}}{M_{\odot}}. \quad (46)$$

We note that these results do not depend on the specific mass  $m$  and scattering length  $a_s$  of the bosons, but only on the ratio  $a_s/m^3$ . For a ratio  $(a_s/\text{fm})(\text{eV}/mc^2)^3 = 3.28 \times 10^3$ , we obtain  $M_{\max} = 2.03 \times 10^{15} M_{\odot}$  and  $R_{\min} = 609 \text{ pc}$ . The maximum mass is much larger than the typical core mass of a DM halo. Assuming that a self-interacting BEC star at  $T = 0$  describes the quantum core of a DM halo, we conclude that such cores are nonrelativistic since  $M_c \ll M_{\max}$  in general. Since the maximum mass is much larger than the core mass, gravity can be treated within a Newtonian framework.

#### D. Bosonic DM with an attractive self-interaction

We consider a gas of self-interacting bosons at  $T = 0$  forming a BEC. The wavefunction of a self-gravitating BEC with a quartic self-interaction is governed by the GPP equations [6]. The equation of state of a self-interacting BEC is given by Eq. (29). We assume that the self-interaction is attractive ( $a_s < 0$ ). This is the case for the axion [11]. Using Madelung’s hydrodynamic representation of the GPP equations, and taking the quantum potential into account, we find that the fundamental differential equation of quantum hydrostatic equilibrium determining the density profile of the BEC is given by Eq. (31) [6]. This equation can be solved numerically [38]. The density profile of a noninteracting BEC star at  $T = 0$  (ground state) extends to infinity. The mass-radius relation has been obtained in [6, 38]. There is a maximum mass

$$M_{\max}^{\text{exact}} = 1.012 \frac{\hbar}{\sqrt{Gm|a_s|}} \quad (47)$$

corresponding to a minimum stable radius

$$(R_{99}^*)^{\text{exact}} = 5.5 \left( \frac{|a_s| \hbar^2}{Gm^3} \right)^{1/2}. \quad (48)$$

When  $M_c > M_{\max}$  the axion star is expected to collapse and form a dense axion star, a black hole or a bosenova as discussed in [46–54].

#### E. Mass-radius relation of isothermal DM halos

In the previous subsections, we have focused on the quantum core of DM halos. Ultracompact dwarf DM

halos just have a quantum core (ground state). Larger DM halos have a “core-halo” structure with a quantum core surrounded by an atmosphere. We have seen that the structure of the quantum core strongly depends on the nature of the DM particle. By contrast, the structure of the atmosphere is relatively independent of the DM particle. We assume that it has an isothermal equation of state

$$P = \rho \frac{k_B T}{m} \quad (49)$$

with an effective temperature  $T$ . For sufficiently large DM halos, the isothermal atmosphere dominates the core. Indeed, the DM halo mass  $M_h$  is much larger than the core mass  $M_c$  and it is a good approximation to assume that the DM halo is purely isothermal.<sup>8</sup> Therefore, from the “outside”, large DM halos behave as classical isothermal spheres. If  $M_h$  represents the halo mass and  $r_h$  the halo radius as defined in Appendix G, then the mass-radius and temperature-radius relations of isothermal DM halos are [7]

$$M_h = 1.76 \Sigma_0 r_h^2, \quad \frac{k_B T}{m} = 0.954 G \Sigma_0 r_h, \quad (50)$$

where  $\Sigma_0$  is the universal surface density of DM halos given by Eq. (1). On the other hand, the circular velocity at the halo radius is

$$v_h^2 = \frac{G M_h}{r_h} = 1.76 \Sigma_0 G r_h = 1.33 G \Sigma_0^{1/2} M_h^{1/2}. \quad (51)$$

### III. A GENERALIZED WAVE EQUATION

#### A. Coarse-grained dynamics

The previous results can be obtained in a unified manner from the generalized GPP equations [7, 55, 56]

$$i \hbar \frac{\partial \psi}{\partial t} = - \frac{\hbar^2}{2m} \Delta \psi + m \Phi \psi + \frac{K \gamma m}{\gamma - 1} |\psi|^{2(\gamma-1)} \psi + 2k_B T \ln |\psi| \psi - i \frac{\hbar}{2} \xi \left[ \ln \left( \frac{\psi}{\psi^*} \right) - \left\langle \ln \left( \frac{\psi}{\psi^*} \right) \right\rangle \right] \psi, \quad (52)$$

$$\Delta \Phi = 4\pi G |\psi|^2. \quad (53)$$

As discussed in more detail in [7, 55], the thermal ( $T$ ) and dissipative ( $\xi$ ) terms present in the generalized GPP equations (52) and (53) parametrize the complicated processes of violent relaxation [15] and gravitational cooling [16] experienced by a collisionless system of self-gravitating fermions or bosons. As a result, the generalized GPP equations (52) and (53) describe the evolution of the system on a “coarse-grained” scale.

<sup>8</sup> We have in mind, for example, the Medium Spiral ( $R \sim 10 \text{ kpc}$  and  $M \sim 10^{11} M_{\odot}$ ).

## B. Madelung transformation

Making the Madelung transformation

$$\psi(\mathbf{r}, t) = \sqrt{\rho(\mathbf{r}, t)} e^{iS(\mathbf{r}, t)/\hbar}, \quad (54)$$

$$\rho = |\psi|^2, \quad \mathbf{u} = \frac{\nabla S}{m}, \quad (55)$$

we can show that the generalized GPP equations (52) and (53) are equivalent to the fluid equations

$$\frac{\partial \rho}{\partial t} + \nabla \cdot (\rho \mathbf{u}) = 0, \quad (56)$$

$$\frac{\partial \mathbf{u}}{\partial t} + (\mathbf{u} \cdot \nabla) \mathbf{u} = -\frac{1}{\rho} \nabla P - \nabla \Phi - \frac{1}{m} \nabla Q - \xi \mathbf{u}, \quad (57)$$

$$\Delta \Phi = 4\pi G \rho, \quad (58)$$

where

$$Q = -\frac{\hbar^2}{2m} \frac{\Delta \sqrt{\rho}}{\sqrt{\rho}} \quad (59)$$

is the quantum potential and  $P$  is the pressure determined by the equation of state

$$P = K \rho^\gamma + \rho \frac{k_B T}{m} \quad (\gamma = 1 + 1/n). \quad (60)$$

This equation of state has a linear part and a polytropic part. The linear (isothermal) equation of state accounts for effective thermal effects. The polytropic equation of state takes into account the self-interaction of the bosons or the quantum pressure arising from the Pauli exclusion principle for fermions. The equation of state (60) defines a composite model of DM halos with a core-halo structure. The polytropic equation of state dominates in the core where the density is high and the isothermal equation of state dominates in the halo where the density is low (we assume that  $\gamma > 1$ ). As a result, the corresponding DM halos present a quantum (fermionic/bosonic) core surrounded by an isothermal envelope. The quantum core solves the cusp problem and the isothermal envelope leads to flat rotation curves. This model has been studied in detail in [7] for self-interacting BECs. Its extension to noninteracting BECs and fermions is under progress.

## C. Condition of quantum hydrostatic equilibrium

The equilibrium state of the hydrodynamic equations (56) and (57) satisfies the condition of quantum hydrostatic equilibrium [55]

$$\frac{\rho}{m} \nabla Q + \nabla P + \rho \nabla \Phi = \mathbf{0}. \quad (61)$$

It describes the balance between the quantum potential arising from the Heisenberg uncertainty principle, the quantum pressure (due to Pauli exclusion principle for fermions or due to the self-interaction of bosons), the pressure due to the effective temperature, and the gravitational attraction. Combining Eq. (61) with the Poisson equation (58), we obtain the fundamental differential equation of quantum hydrostatic equilibrium [55]

$$\frac{\hbar^2}{2m^2} \Delta \left( \frac{\Delta \sqrt{\rho}}{\sqrt{\rho}} \right) - \nabla \cdot \left( \frac{\nabla P}{\rho} \right) = 4\pi G \rho. \quad (62)$$

For the equation of state (60), it takes the form

$$\frac{\hbar^2}{2m^2} \Delta \left( \frac{\Delta \sqrt{\rho}}{\sqrt{\rho}} \right) - \frac{K\gamma}{\gamma-1} \Delta \rho^{\gamma-1} - \frac{k_B T}{m} \Delta \ln \rho = 4\pi G \rho. \quad (63)$$

This differential equation determines the general equilibrium density profile  $\rho(\mathbf{r})$  of a quantum DM halo in our model [7, 55]. This profile generically has a core-halo structure with a polytropic core and an isothermal halo.

In the core, the differential equation (63) reduces to

$$\frac{\hbar^2}{2m^2} \Delta \left( \frac{\Delta \sqrt{\rho}}{\sqrt{\rho}} \right) - \frac{K\gamma}{\gamma-1} \Delta \rho^{\gamma-1} = 4\pi G \rho. \quad (64)$$

It determines the structure of the quantum core as described in Secs. II A-II D.

In the halo, the differential equation reduces to

$$-\frac{k_B T}{m} \Delta \ln \rho = 4\pi G \rho. \quad (65)$$

It is equivalent to the Emden equation [35]. It determines the structure of the isothermal atmosphere of large DM halos as described in Sec. II E.

## D. Free energy

The free energy associated with the generalized GPP equations (52) and (53) or equivalently with the hydrodynamic equations (56) and (57) is

$$F = E_* - TS = \Theta_c + \Theta_Q + U + W - TS. \quad (66)$$

The energy  $E_*$  is the sum of the classical kinetic energy

$$\Theta_c = \int \rho \frac{\mathbf{u}^2}{2} d\mathbf{r}, \quad (67)$$

the quantum kinetic energy

$$\Theta_Q = \frac{\hbar^2}{8m^2} \int \frac{(\nabla \rho)^2}{\rho} d\mathbf{r}, \quad (68)$$

the internal energy associated with the polytropic equation of state

$$U = \frac{K}{\gamma-1} \int \rho^\gamma d\mathbf{r}, \quad (69)$$



and the gravitational energy

$$W = \frac{1}{2} \int \rho \Phi d\mathbf{r}. \quad (70)$$

On the other hand,

$$S = -k_B \int \frac{\rho}{m} (\ln \rho - 1) d\mathbf{r} \quad (71)$$

is the Boltzmann entropy associated with the isothermal equation of state.

The generalized GPP equations (52) and (53) or equivalently the hydrodynamic equations (56) and (57) satisfy an  $H$ -theorem [55]

$$\dot{F} = -\xi \int \rho \mathbf{u}^2 d\mathbf{r} = -2\xi \Theta_c \leq 0. \quad (72)$$

The free energy cannot increase. At equilibrium, we have  $\dot{F} = 0$  implying  $\mathbf{u} = \mathbf{0}$ . Then, Eq. (57) leads to the condition of quantum hydrostatic equilibrium (61). When  $\xi > 0$ , using Lyapunov's direct method, one can show that the system relaxes, for  $t \rightarrow +\infty$ , towards a stable equilibrium state which is a (local) minimum of free energy at fixed mass.

The extremization of the free energy at fixed mass, corresponding to the variational principle  $\delta F - \frac{\mu}{m} \delta M = 0$  where  $\mu$  is a Lagrange multiplier, returns the condition of quantum hydrostatic equilibrium (61). Furthermore, (local) minima of free energy are stable while maxima or saddle points are unstable.

The generalized GPP equations (52) and (53) are associated with a canonical description in which the temperature  $T$  is fixed. It is possible to modify these equations so that the temperature  $T(t)$  evolves in time in order to conserve the energy (see Appendix I of [55]). This corresponds to a microcanonical description. As is well-known, the equilibrium states are the same in the microcanonical and canonical ensembles. However, their stability may be different in case of ensembles inequivalence. In particular, equilibrium states that are unstable in the canonical ensemble may be stable in the microcanonical (this is because the microcanonical ensemble is more constrained than the canonical ensemble). For example, equilibrium states with a negative specific heat are always unstable in the canonical ensemble while they may be stable in the microcanonical ensemble.

#### IV. ANALYTICAL MODEL OF DM HALOS WITH A POLYTROPIC CORE AND AN ISOTHERMAL ATMOSPHERE

In this section, we develop an approximate analytical model of DM halos with a polytropic core surrounded by an isothermal atmosphere. For simplicity, we assume that the density of the isothermal atmosphere is uniform. In all the DM models discussed in Sec. II the quantum core can be described by a polytropic equation of

state. Therefore, by considering a polytropic core with an arbitrary index  $n$ , we can account for a wide diversity of situations and, in particular, unify the treatment of fermionic and bosonic DM halos. We shall enclose the system within a box of radius  $R$ . The box is necessary to have a finite mass  $M$ . In order to connect this model with real DM halos, we shall identify the box radius  $R$  with the halo radius  $r_h$  and the mass  $M$  with the halo mass  $M_h$ . Therefore, we set

$$M = M_h, \quad R = r_h. \quad (73)$$

The mass and the radius of sufficiently large DM halos are related to each other by the first relation of Eq. (50).

##### A. Polytropic core

We modelize the core of a DM halo by a pure polytrope of index  $n$ . Its mass  $M_c$  and its radius  $R_c$  satisfy the mass-radius relation [35]

$$M_c^{(n-1)/n} R_c^{(3-n)/n} = \frac{K(n+1)}{G(4\pi)^{1/n} \omega_n^{(n-1)/n}}. \quad (74)$$

The internal energy and the gravitational energy of the polytropic core are given by (see Appendices B and C)

$$U_c = \frac{n}{5-n} \frac{GM_c^2}{R_c}, \quad W_c = -\frac{3}{5-n} \frac{GM_c^2}{R_c}. \quad (75)$$

Therefore, its total energy  $E_c = U_c + W_c$  is

$$E_c = -\frac{3-n}{n} U_c = \frac{3-n}{3} W_c = -\frac{3-n}{5-n} \frac{GM_c^2}{R_c}. \quad (76)$$

Combined with Eq. (74), we obtain

$$E_c = -\frac{3-n}{5-n} \left[ \frac{(4\pi)^{1/n}}{n+1} \right]^{n/(3-n)} \frac{1}{\omega_n^{(n-1)/(3-n)}} \times \frac{G^{3/(3-n)} M_c^{(5-n)/(3-n)}}{K^{n/(3-n)}}. \quad (77)$$

##### B. Isothermal atmosphere of uniform density

We modelize the halo by an isothermal atmosphere of mass  $M_a = M - M_c$  contained between the spheres of radius  $R_c$  and  $R$ . The internal energy of a gas with the isothermal equation of state (49) is [55]

$$U = \frac{k_B T}{m} \int \rho (\ln \rho - 1) d\mathbf{r}. \quad (78)$$

It can be written as  $U = -TS_B$  where  $S_B = -k_B \int (\rho/m) (\ln \rho - 1) d\mathbf{r}$  is the Boltzmann entropy. For a uniform density, we obtain

$$U_a = \frac{k_B T}{m} (M - M_c) [\ln(M - M_c) - \ln V - 1], \quad (79)$$

where  $V = (4/3)\pi R^3$  is the total volume of the system. On the other hand, the gravitational energy of the uniform atmosphere in the presence of the “external” polytropic core is given by (see Appendix F)

$$W_a = -\frac{3GM_c(M - M_c)}{2R} - \frac{3G(M - M_c)^2}{5R}. \quad (80)$$

To obtain these results, we have assumed that  $R_c \ll R$  which is a very good approximation in all cases of physical interest.

### C. Free energy

Using the foregoing results, the total free energy of the system (core + halo) is

$$F = -\frac{3-n}{5-n} \frac{GM_c^2}{R_c} + \frac{k_B T}{m} (M - M_c) [\ln(M - M_c) - \ln V - 1] - \frac{3GM_c(M - M_c)}{2R} - \frac{3G(M - M_c)^2}{5R}. \quad (81)$$

For a given value of  $M$ ,  $R$  and  $T$ , the free energy is a function  $F(M_c)$  of the core mass. The extrema of this function determine the possible equilibrium states of the system. More precisely, they determine the possible equilibrium core masses  $M_c^{(i)}$  as a function of  $M$ ,  $R$  and  $T$ . This is valid both in the canonical and in the microcanonical ensembles. Indeed, the extrema of  $F(M_c)$  coincide with the extrema of  $S(M_c)$  at fixed energy. In the canonical ensemble, a minimum of  $F(M_c)$  corresponds to a stable equilibrium state (most probable state) while a maximum of  $F(M_c)$  corresponds to an unstable equilibrium state (less probable state). In the microcanonical ensemble, a maximum of  $S(M_c)$  at fixed energy corresponds to a stable equilibrium state (most probable state) while a minimum of  $S(M_c)$  at fixed energy corresponds to an unstable equilibrium state (less probable state). In this paper, we only consider the canonical ensemble. The microcanonical ensemble can be studied along the same lines (see [33]).

It is convenient to introduce the dimensionless quantities

$$x = \frac{M_c}{M}, \quad \eta = \frac{\beta G M m}{R}, \quad (82)$$

$$f(x) = \frac{F(M_c)R}{GM^2}, \quad (83)$$

and

$$\nu = \left[ \frac{G}{K(n+1)} \right]^{n/(3-n)} (4\pi)^{1/(3-n)} \frac{1}{\omega_n^{(n-1)/(3-n)}} \times RM^{(n-1)/(3-n)}, \quad (84)$$

so that Eq. (81) can be rewritten as

$$f(x) = -\frac{3-n}{5-n} \nu x^{(5-n)/(3-n)} + \frac{1}{\eta} (1-x) \left[ \ln \left( \frac{M}{V} \right) + \ln(1-x) - 1 \right] - \frac{3}{2} x(1-x) - \frac{3}{5} (1-x)^2 \quad (85)$$

with  $0 \leq x \leq 1$ .

### D. Connection to DM halos

Before going further let us connect the dimensionless variables introduced previously to the parameters of the DM halos. The variable  $x$  represents the normalized core mass. Using Eq. (73) it can be written as

$$x = \frac{M_c}{M_h}. \quad (86)$$

The variable  $\eta$  represents the normalized inverse temperature. For DM halos, using Eqs. (50) and (73), we get

$$\eta = \frac{\beta G M_h m}{r_h} = 1.84. \quad (87)$$

We see that the normalized inverse temperature is of order 2. This is essentially a consequence of the virial theorem. Since our approach is approximate, we will allow  $\eta$  to vary slightly around this value. Finally, the variable  $\nu$  characterizes the mass  $M_h$  of the DM halos. For fermionic DM halos, we have

$$\nu_F = 8 \left( \frac{4\pi^2}{3} \right)^{2/3} \frac{1}{\omega_{3/2}^{1/3}} \frac{Gm^{8/3}}{h^2} RM^{1/3}. \quad (88)$$

This parameter is related to the “degeneracy parameter”  $\mu$  introduced in [57] (we have  $\nu_F \propto \mu^{2/3}$ ). Using Eqs. (50) and (73), we get

$$\nu_F = 8 \left( \frac{4\pi^2}{3} \right)^{2/3} \frac{1}{\omega_{3/2}^{1/3}} \frac{Gm^{8/3}}{h^2} \frac{1}{\sqrt{1.76} \Sigma_0} M_h^{5/6}. \quad (89)$$

For noninteracting BECDM halos, we have

$$\nu_B = \frac{2}{\omega_2} \frac{Gm^2}{h^2} RM. \quad (90)$$

Using Eqs. (50) and (73), we get

$$\nu_B = \frac{2}{\omega_2} \frac{Gm^2}{h^2} \frac{1}{\sqrt{1.76} \Sigma_0} M_h^{3/2}. \quad (91)$$

For self-interacting BECDM halos in the TF limit, we have

$$\nu_{TF} = \left( \frac{Gm^3}{a_s h^2} \right)^{1/2} R. \quad (92)$$

This parameter is related to the parameter  $\mu$  introduced in [7] (we have  $\nu_{\text{TF}} \propto \mu^{1/2}$ ). Using Eqs. (50) and (73), we get

$$\nu_{\text{TF}} = \left( \frac{Gm^3}{a_s \hbar^2} \right)^{1/2} \frac{1}{\sqrt{1.76 \Sigma_0}} M_h^{1/2}. \quad (93)$$

### E. Equilibrium states

The equilibrium states, corresponding to  $f'(x) = 0$ , are the solutions of the equation

$$\ln(1-x) - \frac{9}{5}x\eta + \frac{3}{10}\eta + \ln\left(\frac{M}{V}\right) + \nu\eta x^{2/(3-n)} = 0. \quad (94)$$

This equation determines the normalized core mass  $x = M_c/M$  as a function of  $\eta$ ,  $\nu$  and  $M/V$ . For  $x = 0$  (gaseous phase) we find  $\eta(0) = -(10/3) \ln(M/V) \equiv \eta_0$ . Setting

$$\ln\left(\frac{M}{V}\right) = -\frac{3}{10}\eta_0, \quad (95)$$

we can rewrite Eq. (94) as

$$\ln(1-x) + \nu\eta x^{2/(3-n)} - \frac{9}{5}x\eta + \frac{3}{10}(\eta - \eta_0) = 0. \quad (96)$$

The solutions of this equation can be easily found by studying the inverse function

$$\eta(x) = \frac{\eta_0 - \frac{10}{3} \ln(1-x)}{1 + \frac{10}{3} \left[ \nu x^{2/(3-n)} - \frac{9}{5}x \right]} \quad (97)$$

for a given value of  $\nu$  (see Fig 4). Our analytical model is valid for sufficiently large values of  $\nu$  (corresponding to large DM halos). On the other hand, the results depend on the value of  $n$ . In the following, we assume  $1 < n < 3$ .<sup>9</sup> For  $x \rightarrow 0$ , we get

$$\eta(x) = \eta_0 + \left( 6\eta_0 + \frac{10}{3} \right) x + \dots \quad (98)$$

Close to  $x = 0$ , the curve  $\eta(x)$  is always increasing. For  $x \rightarrow 1$ , we get

$$\eta \sim \frac{-\ln(1-x)}{\nu - \frac{3}{2}} \rightarrow +\infty, \quad (99)$$

where we have assumed  $\nu > 3/2$  in order to avoid unphysical results due to the invalidity of our model for small values of  $\nu$ .

We note that the inverse temperature  $\eta(x)$  becomes infinite at some  $x_i \neq 1$  when the denominator in Eq. (97) vanishes, i.e., when

$$1 + \frac{10}{3} \left[ \nu x_i^{2/(3-n)} - \frac{9}{5}x_i \right] = 0. \quad (100)$$

Instead of solving Eq. (100) for  $x_i$  as a function of  $\nu$ , it is simpler to study the inverse function

$$\nu(x_i) = \frac{\frac{9}{5}x_i - \frac{3}{10}}{x_i^{2/(3-n)}}. \quad (101)$$

This function (not represented) has the following properties: (i)  $\nu(x_i)$  is positive provided that  $x_i \geq 1/6$ ; (ii)  $\nu(1) = 3/2$ ; (iii) there is a maximum

$$\nu_* = \frac{3(3-n)}{10(n-1)} [3(n-1)]^{2/(3-n)} \quad (102)$$

at  $(x_i)_* = 1/[3(n-1)]$ . In order to avoid unphysical results related to the divergence of the inverse temperature at some  $x_i \neq 1$ , we assume that  $\nu > \nu_*$ . We find  $\nu_* = 2.7$  for  $n = 2$  and  $\nu_* = 1.545$  for  $n = 3/2$ . In a sense, this critical value  $\nu_*$  is the counterpart of the canonical critical point that appears in the exact caloric curve of self-gravitating fermions and bosons (see Fig. 32 of [57] for fermions), although it manifests itself in a singular manner in our simple analytical model.

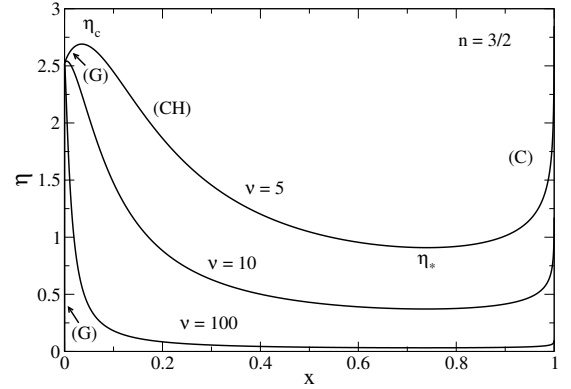


FIG. 4: The function  $\eta(x)$  for different values of  $\nu$  and for  $n = 3/2$  (the figure for  $n = 2$  is similar). We have indicated the gaseous phase (G), the condensed phase (C) and the core-halo phase (CH) on the curve corresponding to  $\nu = 5$ .

When  $\nu > \nu_*$  the curve  $\eta(x)$  presents a maximum at  $(x_c(\nu), \eta_c(\nu))$  and a minimum at  $(x_*(\nu), \eta_*(\nu))$ . They are determined by the equations

$$\ln(1-x_e) + \frac{1}{1-x_e} \frac{\frac{3}{10} + \nu x_e^{2/(3-n)} - \frac{9}{5}x_e}{\frac{2}{3-n} \nu x_e^{(n-1)/(3-n)} - \frac{9}{5}} - \frac{3}{10}\eta_0 = 0 \quad (103)$$

and

$$\eta_e = \frac{\eta_0 - \frac{10}{3} \ln(1-x_e)}{1 + \frac{10}{3} \left[ \nu x_e^{2/(3-n)} - \frac{9}{5}x_e \right]}. \quad (104)$$

Instead of solving Eq. (103) for  $x_e$  as a function of  $\nu$ , it is simpler to study the inverse function

$$\nu(x_e) = \frac{\frac{3}{10} - \frac{9}{5}x_e + \frac{9}{5} \left[ \frac{3}{10}\eta_0 - \ln(1-x_e) \right] (1-x_e)}{(1-x_e) \left[ \frac{3}{10}\eta_0 - \ln(1-x_e) \right] \frac{2}{3-n} x_e^{\frac{n-1}{3-n}} - x_e^{\frac{2}{3-n}}}. \quad (105)$$

<sup>9</sup> The index  $n = 1$  is special and has been treated in [7]. The condition  $n < 3$  is required in order to have a stable core [35].

The values of  $(x_c, \eta_c)$  and  $(x_*, \eta_*)$  characterizing the maximum and the minimum of the curve  $\eta(x)$  as a function of  $\nu$  (see Fig. 4) are plotted in Figs. 5 and 6. We note that  $\eta_c(\nu)$  and  $\eta_*(\nu)$  decrease as  $\nu$  increases. This is consistent with the properties of the exact caloric curve of self-gravitating fermions (see Fig. 34 in [57]).

For  $\nu \rightarrow +\infty$ , we find that

$$x_c \sim \left[ \frac{3-n}{2} \left( \frac{9}{5} + \frac{1}{\eta_0} \right) \frac{1}{\nu} \right]^{(3-n)/(n-1)} \rightarrow 0 \quad (106)$$

and

$$\eta_c \rightarrow \eta_0. \quad (107)$$

Therefore, we can identify  $\eta_0$  with the critical inverse temperature of a purely isothermal ( $x = 0$ ) self-gravitating gas confined within a box [57], i.e., we set

$$\eta_0 = 2.52. \quad (108)$$

On the other hand, for  $\nu \rightarrow +\infty$ , we find that  $x_* \rightarrow x_*^c$ , where  $x_*^c$  is the solution of the equation

$$\ln(1 - x_*^c) + \frac{3-n}{2} \frac{x_*^c}{1 - x_*^c} - \frac{3}{10} \eta_0 = 0. \quad (109)$$

We numerically obtain  $x_*^c \simeq 0.7355$  for  $n = 3/2$  and  $x_*^c \simeq 0.837$  for  $n = 2$ . We then find that

$$\eta_* \sim \frac{3-n}{2\nu} \frac{(x_*^c)^{(1-n)/(3-n)}}{1 - x_*^c} \rightarrow 0. \quad (110)$$

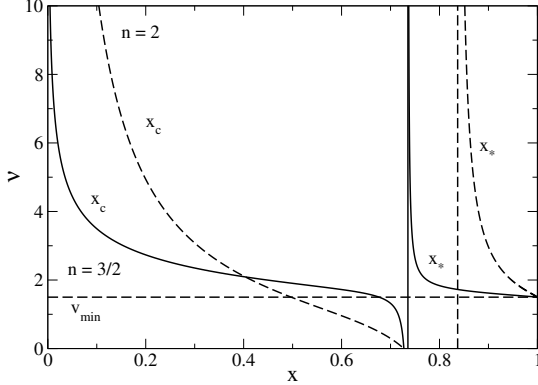


FIG. 5: The functions  $\nu(x_c)$  and  $\nu(x_*)$ . By inversion, they give the values of  $x_c$  and  $x_*$  as a function of  $\nu$ . The solid lines correspond to  $n = 3/2$  and the dashed lines correspond to  $n = 2$ .

### F. Stability of the equilibrium states

Let us now consider more specifically the function  $f(x)$  giving the free energy of the system as a function of the

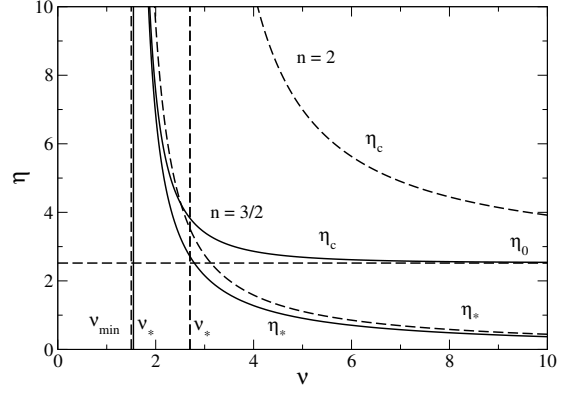


FIG. 6: The values of  $\eta_c$  and  $\eta_*$  as a function of  $\nu$ . The solid lines correspond to  $n = 3/2$  and the dashed lines correspond to  $n = 2$ .

core mass  $x$  for a given value of  $\nu$  and  $\eta$ . Using Eq. (95), we can rewrite Eq. (85) as

$$\begin{aligned} f(x) = & -\frac{3-n}{5-n} \nu x^{(5-n)/(3-n)} \\ & + \frac{1}{\eta} (1-x) \left[ -\frac{3}{10} \eta_0 + \ln(1-x) - 1 \right] \\ & - \frac{3}{2} x(1-x) - \frac{3}{5} (1-x)^2. \end{aligned} \quad (111)$$

Its first derivative is

$$f'(x) = -\nu x^{2/(3-n)} + \frac{3}{10} \frac{\eta_0}{\eta} - \frac{1}{\eta} \ln(1-x) - \frac{3}{10} + \frac{9}{5} x. \quad (112)$$

The condition  $f'(x) = 0$  determines the possible equilibrium states of the system as we have just seen. The stability of these equilibrium states in the canonical ensemble is then determined by the sign of the second derivative of the free energy:

$$f''(x) = -\nu \frac{2}{3-n} x^{(n-1)/(3-n)} + \frac{1}{\eta(1-x)} + \frac{9}{5}. \quad (113)$$

In the canonical ensemble an equilibrium state is stable when  $f''(x) > 0$ , corresponding to a minimum of free energy, and unstable when  $f''(x) < 0$ , corresponding to a maximum of free energy. In Fig. 7 we have plotted the curve  $f(x)$  in the case  $\eta_* < \eta < \eta_c$  where the system has three equilibrium states as detailed in the following section.

The values of the function  $f(x)$  at  $x = 0$  and  $x = 1$  are

$$f(0) = -\frac{1}{\eta} \left( \frac{3}{10} \eta_0 + 1 \right) - \frac{3}{5} \quad (114)$$

and

$$f(1) = -\frac{3-n}{5-n} \nu. \quad (115)$$

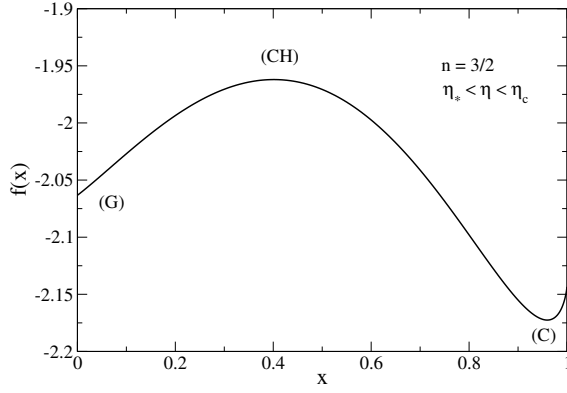


FIG. 7: The function  $f(x)$  for  $\eta_* < \eta < \eta_c$  (specifically  $n = 3/2$ ,  $\nu = 5$  and  $\eta = 1.2$ ).

For  $x \rightarrow 0$ , we find that

$$f(x) = f(0) + \frac{3}{10} \left( \frac{\eta_0}{\eta} - 1 \right) x + \dots \quad (116)$$

The term in parenthesis is positive when  $\eta < \eta_0$  and negative when  $\eta > \eta_0$ . Since the function  $f(x)$  is defined for  $x \geq 0$ , and since the slope of the function  $f(x)$  at  $x = 0$  is positive when  $\eta < \eta_0$ , the solution  $x = 0$  (gaseous phase) is a local minimum of  $f(x)$  in that case even though  $f'(0) \neq 0$ . We shall therefore consider that the solution  $x = 0$  is a stable equilibrium state when  $\eta < \eta_0$ . When  $\eta_0 < \eta < \eta_c$ , the function  $f(x)$  admits a local minimum ( $f'(x_1) = 0$  and  $f''(x_1) > 0$ ) at some  $x_1 > 0$ . This is consistent with the fact that the slope of the function  $f(x)$  at  $x = 0$  is negative in that case. We note that  $x_1$  is always very close to zero in practice so that the function  $f(x)$  always look like Fig. 7 when  $\eta_* < \eta < \eta_c$ .

### G. The different equilibrium states

After the mathematical preliminaries, we are now ready to perform the complete analysis of the equilibrium states of our simple analytical model. As explained previously we assume  $\nu > \nu_*$ .

The curve  $\eta(x)$  is made of a vertical branch at  $x = 0$  up to  $\eta = \eta_0$ , then it increases, reaches a maximum  $\eta_c$  at  $x_c$ , decreases, reaches a minimum  $\eta_*$  at  $x_*$ , and finally increases up to infinity when  $x \rightarrow 1$  (see Fig. 4). When  $\eta < \eta_*$ , there is a unique equilibrium state ( $x = 0$ ). It corresponds to the gaseous phase (G). When  $\eta > \eta_c$ , there is a unique equilibrium state ( $x \simeq 1$ ). It corresponds to the condensed phase (C). They are both stable (minima of free energy). When  $\eta_* < \eta < \eta_c$  there are three equilibrium states (see Fig. 7): (i) a gaseous phase (G); (ii) a core-halo phase (CH); (iii) a condensed phase (C). Let us analyze these solutions in more detail in the limit  $\nu \rightarrow +\infty$  with  $\eta < \eta_0$ :

(i) The gaseous solution (G) corresponds to a purely isothermal halo without core. The core mass is equal to zero:  $x_G = 0$ . This solution is stable, being a minimum of free energy, although the derivative of  $f(x)$  does not vanish at  $x = 0$  as explained above.

(ii) The core-halo solution (CH) corresponds to an isothermal halo harboring a core with a small mass ( $x_{CH} \ll 1$ ). From Eq. (96), we find that the normalized core mass scales as

$$x_{CH} \sim \left[ \frac{3}{10} \frac{\eta_0 - \eta}{\eta} \frac{1}{\nu} \right]^{(3-n)/2}. \quad (117)$$

Substituting Eq. (117) into Eq. (113) we find that

$$f''(x_{CH}) \sim -\frac{2}{3-n} \left[ \frac{3}{10} \frac{\eta_0 - \eta}{\eta} \right]^{(n-1)/2} \nu^{(3-n)/2} \rightarrow -\infty. \quad (118)$$

Therefore, the core-halo solution is unstable in the canonical ensemble being a maximum of free energy. It is similar to a “germ” or a “critical droplet” in the language of phase transitions. It has a negative specific heat [7]. It may, however, be stable in the microcanonical ensemble which is physically more relevant than the canonical ensemble (see the discussion in [7]). In the following, we shall assume that the core-halo state is stable in the microcanonical ensemble (being an entropy maximum) or, at least, that it has a very long lifetime.

(iii) The condensed solution (C) corresponds to a quantum core surrounded by a tenuous atmosphere ( $x_C \sim 1$ ). From Eq. (96), we find that the normalized core mass scales as

$$1 - x_C \propto e^{-\eta\nu}, \quad (119)$$

showing that the quantum core contains almost all the mass. Substituting Eq. (119) into Eq. (113) we find that

$$f''(x_C) \propto \frac{1}{\eta} e^{\eta\nu} \rightarrow +\infty. \quad (120)$$

Therefore, the condensed solution is stable being a minimum of free energy.

The gaseous solutions (G) constitute the lower branch of the generic phase diagram  $M_c(M_h)$  reported in Fig. 49 of [7]. The core-halo solutions (CH) constitute the upper branch of this phase diagram that appears above a canonical critical point (bifurcation point)  $(M_h)_{CCP}$  here identified with  $\nu_*$ . This is the branch of most physical interest in the physics of DM halos. The core mass – halo mass relation on the core-halo branch (CH) is studied in detail in the following sections.

## V. JUSTIFICATION OF THE VELOCITY DISPERSION TRACING RELATION AND DETERMINATION OF THE $M_c(M_v)$ RELATION

### A. The velocity dispersion tracing relation

We consider the core-halo solution (CH) of Sec. IV G. The normalized core mass is given by Eq. (117). We

first show that this result is equivalent to the “velocity dispersion tracing” relation [7, 34]

$$v_c^2 \sim v_h^2 \quad \text{or} \quad M_c \sim \frac{R_c}{r_h} M_h, \quad (121)$$

stating that the velocity dispersion in the core  $v_c^2 \sim GM_c/R_c$  is of the same order as the velocity dispersion in the halo  $v_h^2 \sim GM_h/r_h$ . Using Eq. (74), this relation can be rewritten as

$$M_c \sim \left[ \frac{K(n+1)}{G} \right]^{n/2} \frac{\omega_n^{(n-1)/2}}{(4\pi)^{1/2}} \left( \frac{M_h}{r_h} \right)^{(3-n)/2}. \quad (122)$$

On the other hand, using Eqs. (82) and (84), we find that Eq. (117) is equivalent to

$$M_c \sim \left[ \frac{3}{10} \frac{\eta_0 - \eta}{\eta} \right]^{(3-n)/2} \left[ \frac{K(n+1)}{G} \right]^{n/2} \frac{\omega_n^{(n-1)/2}}{(4\pi)^{1/2}} \times \left( \frac{M_h}{r_h} \right)^{(3-n)/2} \quad (123)$$

The formulae (122) and (123) are consistent with each other up to a multiplicative factor of order unity. They exactly coincide if we take

$$\eta = \frac{3}{13} \eta_0 = 0.582. \quad (124)$$

As a result, Eq. (117) is equivalent to the “velocity dispersion tracing” relation from Eq. (121). Our study provides therefore a justification of this relation from (effective) thermodynamical arguments.

### B. The $M_c(M_h)$ relation

If we now substitute the relation  $M_h = 1.76 \Sigma_0 r_h^2$  from Eq. (50) into Eq. (122) we obtain

$$M_c \sim \left[ \frac{K(n+1)}{G} \right]^{n/2} \frac{\omega_n^{(n-1)/2}}{(4\pi)^{1/2}} (1.76 \Sigma_0 M_h)^{(3-n)/4}. \quad (125)$$

This equation gives the relation between the core mass  $M_c$  and the halo mass  $M_h$ . It displays the fundamental scaling

$$M_c \propto M_h^{(3-n)/4}. \quad (126)$$

Combining Eq. (125) with the minimum halo mass from Eq. (G6), we get

$$\frac{M_c}{(M_h)_{\min}} \sim A_n \left[ \frac{M_h}{(M_h)_{\min}} \right]^{(3-n)/4}, \quad (127)$$

where

$$A_n = \left( \frac{1.76}{4\pi} \right)^{(3-n)/4} \frac{\xi_1^{(n+1)/2} (-\theta'_1)^{(n-1)/2}}{\xi_h^{(3n-1)/4} (-\theta'_h)^{(n+1)/4}} \quad (128)$$

is a constant of order unity.

### C. The $M_c(M_v)$ relation

Following our previous work [7], we have defined the halo mass  $M_h$  and the halo radius  $r_h$  such that  $r_h$  represents the distance at which the central density is divided by 4 (see Appendix G). However, Schive *et al.* [26] use another definition of the halo mass  $M_v$  and halo radius  $r_v$ . They are connected by

$$M_v = \frac{4}{3} \pi r_v^3 \zeta(0) \rho_{m,0} \quad (129)$$

where  $\rho_{m,0} = \Omega_{m,0} \epsilon_0 / c^2$  is the present background matter density in the Universe and  $\zeta(0)$  is a prefactor of order  $\sim 350$ . For the numerical applications, we shall take  $\Omega_{m,0} = 0.3089$  and  $\epsilon_0 / c^2 = 8.62 \times 10^{-24} \text{ g m}^{-3}$  giving  $\rho_{m,0} = 2.66 \times 10^{-24} \text{ g m}^{-3}$  [2]. Using

$$\frac{GM_v}{r_v} \sim \frac{GM_h}{r_h}, \quad (130)$$

in consistency with Eq. (121), and Eqs. (50) and (129), we obtain

$$M_h \sim \frac{1}{1.76 \Sigma_0} \left[ \frac{4}{3} \pi \zeta(0) \rho_{m,0} \right]^{2/3} M_v^{4/3}. \quad (131)$$

The scaling  $M_h \propto M_v^{4/3}$  was previously noted in [7]. Normalizing the halo mass by the minimum halo mass, we get

$$\frac{M_h}{(M_h)_{\min}} \sim B_n \left[ \frac{M_v}{(M_h)_{\min}} \right]^{4/3} \quad (132)$$

with

$$B_n = \frac{1}{1.76 \Sigma_0} \left[ \frac{4}{3} \pi \zeta(0) \rho_{m,0} \right]^{2/3} (M_h)_{\min}^{1/3}. \quad (133)$$

Combining Eqs. (127) and (132), we finally obtain the core mass – halo mass relation

$$\frac{M_c}{(M_h)_{\min}} \sim A_n B_n^{(3-n)/4} \left[ \frac{M_v}{(M_h)_{\min}} \right]^{(3-n)/3}. \quad (134)$$

It exhibits the fundamental scaling  $M_c \sim M_v^{(3-n)/3}$ .

*Remark:* Since  $B_n$  is a dimensionless constant of order  $10^{-3}$  (see below), Eq. (133) provides a relation between the DM particle parameters  $(m, a_s)$  [via  $(M_h)_{\min}$ ], the universal DM surface density  $\Sigma_0$  and the present density of matter in the Universe  $\rho_{m,0}$ . Expressing  $\Sigma_0$  and  $\rho_{m,0}$  in terms of the cosmological constant  $\Lambda$ , we will be able (see Sec. VI) to obtain the DM particle parameters  $(m, a_s)$  in terms of the fundamental constants of physics.

## VI. APPLICATION TO QUANTUM MODELS OF DM HALOS

We now apply these results to quantum models of DM halos made of fermions, noninteracting bosons, and self-interacting bosons as described in Sec. II. For reasons that will become clear below, we treat the case of noninteracting bosons first.

### A. Noninteracting bosons

A noninteracting self-gravitating BEC ( $a_s = 0$ ) is equivalent to a polytrope of index  $n = 2$  with a polytropic constant given by Eq. (E3) (see Sec. II B and Appendix E). Using Eqs. (127), (128) and the results of Appendix G, we get

$$\frac{M_c}{(M_h)_{\min}} \sim 1.84 \left[ \frac{M_h}{(M_h)_{\min}} \right]^{1/4}. \quad (135)$$

On the other hand, using Eqs. (26) and (133), we find that

$$\begin{aligned} B_2 &= \frac{1}{1.76 \Sigma_0} \left[ \frac{4}{3} \pi \zeta(0) \rho_{m,0} \right]^{2/3} (1.61)^{1/3} \left( \frac{\hbar^4 \Sigma_0}{G^2 m^4} \right)^{1/9} \\ &= 2.04 \times 10^{-3}. \end{aligned} \quad (136)$$

Therefore, Eq. (132) takes the form

$$\frac{M_h}{(M_h)_{\min}} \sim 2.04 \times 10^{-3} \left[ \frac{M_v}{(M_h)_{\min}} \right]^{4/3}. \quad (137)$$

Combining Eqs. (135) and (137), we obtain the core mass – halo mass relation

$$\frac{M_c}{(M_h)_{\min}} \sim 0.391 \left[ \frac{M_v}{(M_h)_{\min}} \right]^{1/3}. \quad (138)$$

It exhibits the fundamental scaling  $M_c \propto M_v^{1/3}$ . This theoretical scaling is consistent with the scaling found numerically by Schive *et al.* [26]. These authors also presented an heuristic argument to justify this relation. As discussed in Refs. [7, 34], their argument is equivalent to assuming the velocity dispersion tracing relation (121). We stress, however, that this relation is not obvious *a priori* and that other relations, such as the energy tracing relation, could be contemplated as well [34]. They would lead to different results. The fact that the velocity dispersion tracing relation (121) can be justified from a free energy extremization principle, as shown in the present paper, may provide a physical basis for it.

On the other hand, reversing Eq. (136) following the remark at the end of Sec. V C, we get

$$m = \frac{(1.61)^{3/4}}{(1.76)^{9/4}} \left[ \frac{4}{3} \pi \zeta(0) \rho_{m,0} \right]^{3/2} \frac{\hbar}{\Sigma_0^2 G^{1/2} B_2^{9/4}}. \quad (139)$$

The present matter density in the Universe is given by  $\rho_{m,0} = \Omega_{m,0} \epsilon_0 / c^2$  and the density of dark energy is given by  $\rho_\Lambda = \Lambda / 8\pi G = \Omega_{de,0} \epsilon_0 / c^2$  where  $\Omega_{de,0} \simeq 1 - \Omega_{m,0} = 0.6911$  is the present fraction of dark energy and  $\Lambda = 1.00 \times 10^{-35} \text{ s}^{-2}$  is the cosmological constant. Therefore, we can write the present DM density in terms of the cosmological constant as

$$\rho_{m,0} = \frac{\Omega_{m,0}}{\Omega_{de,0}} \frac{\Lambda}{8\pi G} = 0.0178 \frac{\Lambda}{G}. \quad (140)$$

On the other hand, in the framework of the logotropic model [58–60], we have theoretically predicted that the surface density of the DM halos is constant and that its universal value is given in terms of an effective cosmological constant (whose value is the same as Einstein's cosmological constant) by<sup>10</sup>

$$\Sigma_0 = 0.0207 \frac{c\sqrt{\Lambda}}{G}. \quad (141)$$

Now that this formula has been isolated, we can use it independently from the theory developed in [58–60]. Combining Eqs. (139), (140) and (141) we find that the mass of the noninteracting bosonic particle is given by

$$m = 1.41 \times 10^{11} m_\Lambda, \quad (142)$$

where

$$m_\Lambda = \frac{\hbar\sqrt{\Lambda}}{c^2} = 2.08 \times 10^{-33} \text{ eV}/c^2. \quad (143)$$

This mass scale is often interpreted as the smallest mass of the bosons predicted by string theory [61] or as the upper bound on the mass of the graviton [62].<sup>11</sup> This is also the mass of an hypothetical particle called the cosmon. We see that it fixes the mass scale of the DM particle in the case where it is a noninteracting boson. Nevertheless, there is a huge proportionality factor between them, of the order of  $10^{11}$ . We have also found this result in Appendix F of [60] from considerations based on the Jeans instability. These considerations are further developed in Appendix I and generalized to the case of self-interacting bosons and fermions.

*Remark:* Returning to original variables, and using Eqs. (50), (121) and (E5), the core mass – halo mass relation of DM halos made of noninteracting bosons may be written as

$$M_c \sim 2.29 \left( \frac{\hbar^2 M_h}{G m^2 r_h} \right)^{1/2} \sim 2.64 \left( \frac{\hbar^4 \Sigma_0 M_h}{G^2 m^4} \right)^{1/4} \quad (144)$$

leading to  $M_c \propto M_h^{1/4} \propto M_v^{1/3}$ .

### B. Self-interacting bosons

A self-gravitating BEC with a repulsive self-interaction in the TF limit ( $\hbar = 0$ ) is equivalent to a polytrope of

<sup>10</sup> We emphasize that there is no free parameter in the logotropic model [58–60].

<sup>11</sup> It is simply obtained by equating the Compton wavelength of the particle  $\lambda_C = \hbar/mc$  with the Hubble radius  $R_\Lambda = c/H_0 \sim c/\sqrt{\Lambda}$  (the typical size of the visible Universe) giving  $m_\Lambda = \hbar H_0 / c^2 \sim \hbar\sqrt{\Lambda}/c^2$ . By comparison, if we identify the Compton wavelength  $\lambda_C = \hbar/mc$  with the Schwarzschild radius  $r_S \sim Gm/c^2$  we get the Planck mass  $M_P = (\hbar c/G)^{1/2}$ .

index  $n = 1$  with a polytropic constant given by Eq. (30) (see Sec. II C). Using Eqs. (127), (128) and the results of Appendix G, we get

$$\frac{M_c}{(M_h)_{\min}} \sim 1.16 \left[ \frac{M_h}{(M_h)_{\min}} \right]^{1/2}. \quad (145)$$

On the other hand, using Eqs. (43) and (133), we find that

$$\begin{aligned} B_1 &= \frac{1}{1.76 \Sigma_0} \left[ \frac{4}{3} \pi \zeta(0) \rho_{m,0} \right]^{2/3} (13.0)^{1/3} \left( \frac{a_s \hbar^2 \Sigma_0}{G m^3} \right)^{1/3} \\ &= 3.43 \times 10^{-3}. \end{aligned} \quad (146)$$

Therefore, Eq. (132) takes the form

$$\frac{M_h}{(M_h)_{\min}} \sim 3.43 \times 10^{-3} \left[ \frac{M_v}{(M_h)_{\min}} \right]^{4/3}. \quad (147)$$

Combining Eqs. (145) and (147), we obtain the core mass – halo mass relation

$$\frac{M_c}{(M_h)_{\min}} \sim 6.79 \times 10^{-2} \left[ \frac{M_v}{(M_h)_{\min}} \right]^{2/3}. \quad (148)$$

It exhibits the fundamental scaling  $M_c \propto M_v^{2/3}$ . This is a new theoretical prediction [7] that still has to be tested with direct numerical simulations of self-interacting bosons.

On the other hand, reversing Eq. (146) following the remark at the end of Sec. V C, we get

$$\frac{m^3}{a_s} = \frac{13.0}{(1.76)^3} \left[ \frac{4}{3} \pi \zeta(0) \rho_{m,0} \right]^2 \frac{\hbar^2}{G \Sigma_0^2} \frac{1}{B_1^3}. \quad (149)$$

Using Eqs. (140) and (141) we obtain

$$\frac{a_s}{m^3} = 5.34 \times 10^{-15} \frac{r_\Lambda}{m_\Lambda^3}, \quad (150)$$

where

$$\frac{r_\Lambda}{m_\Lambda^3} = \frac{2Gc^2}{\Lambda \hbar^2} = 6.11 \times 10^{17} \text{ fm (eV/c}^2\text{)}^{-3}. \quad (151)$$

In this expression,  $m_\Lambda$  is the mass of the cosmon given by Eq. (143) and

$$r_\Lambda = \frac{2Gm_\Lambda}{c^2} = 5.51 \times 10^{-96} \text{ m} \quad (152)$$

is the gravitational radius of the cosmon [60].

*Remark:* Returning to original variables, and using Eqs. (33), (50) and (121), the core mass – halo mass relation of DM halos made of self-interacting bosons in the TF limit may be written as

$$M_c \sim \pi \left( \frac{a_s \hbar^2 M_h^2}{G m^3 r_h^2} \right)^{1/2} \sim 4.17 \left( \frac{a_s \hbar^2 \Sigma_0 M_h}{G m^3} \right)^{1/2} \quad (153)$$

leading to  $M_c \propto M_h^{1/2} \propto M_v^{2/3}$ .

## C. Fermions

A fermionic core is equivalent to a polytrope of index  $n = 3/2$  with a polytropic constant given by Eq. (4) (see Sec. II A). Using Eqs. (127), (128) and the results of Appendix G, we get

$$\frac{M_c}{(M_h)_{\min}} \sim 1.50 \left[ \frac{M_h}{(M_h)_{\min}} \right]^{3/8}. \quad (154)$$

On the other hand, using Eqs. (14) and (133), we find that

$$\begin{aligned} B_{3/2} &= \frac{1}{1.76 \Sigma_0} \left[ \frac{4}{3} \pi \zeta(0) \rho_{m,0} \right]^{2/3} (4.47)^{1/3} \left( \frac{\hbar^{12} \Sigma_0^3}{G^6 m^{16}} \right)^{1/15} \\ &= 2.70 \times 10^{-3}. \end{aligned} \quad (155)$$

Therefore, Eq. (132) takes the form

$$\frac{M_h}{(M_h)_{\min}} \sim 2.70 \times 10^{-3} \left[ \frac{M_v}{(M_h)_{\min}} \right]^{4/3}. \quad (156)$$

Combining Eqs. (154) and (156), we obtain the core mass – halo mass relation

$$\frac{M_c}{(M_h)_{\min}} \sim 0.163 \left[ \frac{M_v}{(M_h)_{\min}} \right]^{1/2}. \quad (157)$$

It exhibits the fundamental scaling  $M_c \propto M_v^{1/2}$ . This theoretical scaling, previously given in the form of Eq. (154) in Appendix H of [63], is consistent with the scaling found numerically by Ruffini *et al.* [64] (they find an exponent equal to 0.52 instead of 1/2).

On the other hand, reversing Eq. (155) following the remark at the end of Sec. V C, we get

$$m = \frac{(4.47)^{5/16}}{(1.76)^{15/16}} \left[ \frac{4}{3} \pi \zeta(0) \rho_{m,0} \right]^{5/8} \frac{\hbar^{3/4}}{\Sigma_0^{3/4} G^{3/8}} \frac{1}{B_{3/2}^{15/16}}. \quad (158)$$

Using Eqs. (140) and (141) we obtain

$$m = 3.38 \times 10^4 m_\Lambda^*, \quad (159)$$

where

$$m_\Lambda^* = \left( \frac{\Lambda \hbar^3}{G c^3} \right)^{1/4} = \sqrt{m_\Lambda M_P} = 5.04 \times 10^{-3} \text{ eV/c}^2. \quad (160)$$

To our knowledge, this mass scale has not been introduced before. It is the geometric mean of the cosmon mass  $m_\Lambda$  given by Eq. (143) and the Planck mass  $M_P = (\hbar c/G)^{1/2} = 2.18 \times 10^{-5} \text{ g}$ .<sup>12</sup>

<sup>12</sup> In comparison, using the results of [60], the mass of the electron may be written in terms of the fundamental constants of physics as  $m_e = 1.03 \alpha (m_\Lambda M_P^2)^{1/3} = 9.11 \times 10^{-28} \text{ g}$  where  $\alpha \simeq 1/137$  is the fine structure constant.



*Remark:* Comparing Eqs. (136), (146) and (155), we note that the value of  $B_n$  defined by Eq. (133) is relatively insensitive on the value of the polytropic index  $n$  for the cases contemplated. This is because the parameters have been chosen so that  $(M_h)_{\min}$  typically has a fixed value ( $\sim 10^8 M_\odot$ ).

*Remark:* Returning to original variables, and using Eqs. (6), (50) and (121), the core mass – halo mass relation of DM halos made of fermions may be written as

$$M_c \sim 3.10 \frac{\hbar^{3/2}}{m^2} \left( \frac{M_h}{Gr_h} \right)^{3/4} \sim 3.83 \frac{\hbar^{3/2}}{m^2} \left( \frac{M_h \Sigma_0}{G^2} \right)^{3/8} \quad (161)$$

leading to  $M_c \propto M_h^{3/8} \propto M_v^{1/2}$ .

#### D. Semiclassical limit

It is interesting to study how the mass  $M_c$ , the radius  $R_c$ , the velocity dispersion  $GM_c/R_c$  and the energy  $GM_c^2/R_c$  in the core behave in the semiclassical limit  $\hbar \rightarrow 0$ . For noninteracting bosons, using Eq. (144), we find  $M_c \sim R_c \sim GM_c^2/R_c \sim \hbar \rightarrow 0$  and  $GM_c/R_c \sim 1$ . For self-interacting bosons, using Eq. (153), we find  $M_c \sim R_c \sim GM_c^2/R_c \sim \hbar \rightarrow 0$  and  $GM_c/R_c \sim 1$ . For fermions, using Eq. (161), we find  $M_c \sim R_c \sim GM_c^2/R_c \sim \hbar^{3/2} \rightarrow 0$  and  $GM_c/R_c \sim 1$ .

### VII. GAUSSIAN ANSATZ

In this section, we obtain the core mass – halo mass relation of DM halos by combining the velocity dispersion tracing relation (121) with the approximate core mass-radius relation of a self-gravitating BEC at  $T = 0$  obtained in [6] from a Gaussian ansatz. This allows us to recover the preceding results and to generalize them to the case of a repulsive self-interaction ( $a_s > 0$ ), without making the TF approximation, and to the case of an attractive self-interaction ( $a_s < 0$ ). Throughout this section, we introduce appropriate normalizations in order to clearly see the physical origin of the parameters and be able to refine the numerical applications when more precise data will be available.

#### A. Core mass-radius relation

Using a Gaussian ansatz, it is found in [6] that the approximate mass-radius relation of a self-gravitating BEC at  $T = 0$  (ground state) is given by

$$M_c = \frac{2\sigma}{\nu} \frac{\frac{\hbar^2}{Gm^2 R_c}}{1 - \frac{6\pi\zeta a_s \hbar^2}{\nu Gm^3 R_c^2}} \quad (162)$$

with the coefficients  $\sigma = 3/4$ ,  $\zeta = 1/(2\pi)^{3/2}$  and  $\nu = 1/\sqrt{2\pi}$ . Inversely, the radius can be expressed in terms

of the mass as

$$R_c = \frac{\sigma}{\nu} \frac{\hbar^2}{Gm_c m^2} \left( 1 \pm \sqrt{1 + \frac{6\pi\zeta\nu}{\sigma^2} \frac{GmM_c^2 a_s}{\hbar^2}} \right) \quad (163)$$

with  $+$  when  $a_s > 0$  and with  $\pm$  when  $a_s < 0$ . The results of [6] describe the “minimum halo” (ground state) or the quantum core of larger halos. For noninteracting BECs ( $a_s = 0$ ), the mass-radius relation reduces to

$$M_c = \frac{2\sigma}{\nu} \frac{\hbar^2}{Gm^2 R_c}. \quad (164)$$

In the repulsive case ( $a_s > 0$ ) the mass-radius relation is monotonic (see Fig. 2 of [6]). There is a minimum radius

$$(R_c)_{\min} = \left( \frac{6\pi\zeta}{\nu} \right)^{1/2} \left( \frac{a_s \hbar^2}{Gm^3} \right)^{1/2} \quad (165)$$

corresponding to  $M_c \rightarrow +\infty$  (TF limit). For  $R \gg (R_c)_{\min}$  we are in the noninteracting limit (164). In the attractive case ( $a_s < 0$ ) the mass-radius relation is non-monotonic (see Fig. 3 of [6]). There is a maximum mass

$$(M_c)_{\max} = \left( \frac{\sigma^2}{6\pi\zeta\nu} \right)^{1/2} \frac{\hbar}{\sqrt{Gm|a_s|}} \quad (166)$$

corresponding to the radius

$$(R_c)_* = \left( \frac{6\pi\zeta}{\nu} \right)^{1/2} \left( \frac{|a_s| \hbar^2}{Gm^3} \right)^{1/2}. \quad (167)$$

No equilibrium state exist with a mass  $M_c > (M_c)_{\max}$ . For  $M_c < (M_c)_{\max}$  the branch  $R_c > (R_c)_*$  (corresponding to the solutions (163) with the sign  $+$ ) is stable and the branch  $R_c < (R_c)_*$  (corresponding to the solutions (163) with the sign  $-$ ) is unstable. For  $R \gg (R_c)_*$  we are in the noninteracting limit (164) and for  $R \ll (R_c)_*$  we are in the (unstable) nongravitational limit where

$$M_c = \frac{\sigma}{3\pi\zeta} \frac{mR_c}{|a_s|}. \quad (168)$$

#### B. The minimum halo mass

We first determine the minimum halo mass  $(M_h)_{\min}$ . As explained previously, the minimum halo corresponds to the ground state ( $T = 0$ ) of the self-gravitating BEC. In our approximate approach we write the surface density as

$$\Sigma_0 = \alpha \frac{M_c}{R_c^2}, \quad (169)$$

where  $\alpha$  is a constant of order unity (in the numerical applications we take  $\alpha = 1/1.76$  for the reason explained in footnote 13). Eliminating  $R_c$  between Eqs. (162) and (169), and treating  $\Sigma_0$  as a universal constant, we get

the minimum halo mass  $(M_h)_{\min}$  as a function of  $m$  and  $a_s$  (we recall that  $M_h = M_c$  for the ground state). For noninteracting BECs ( $a_s = 0$ ) we find that the minimum halo mass is

$$(M_h)_{\min,0} = \frac{2^{2/3}\sigma^{2/3}}{\nu^{2/3}\alpha^{1/3}} \left( \frac{\hbar^4 \Sigma_0}{G^2 m^4} \right)^{1/3}. \quad (170)$$

The prefactor is 2.92. This can be compared with Eq. (26). Measuring the DM particle mass in units of  $10^{-22}\text{eV}/c^2$ , we get  $(M_h)_{\min,0} = 2.95 \times 10^8 m^{-4/3} M_\odot$ . In the general case, valid for an arbitrary value of  $a_s$ , we find that the minimum halo mass  $(M_h)_{\min}$  is determined by the equation

$$\frac{a_s}{a_*} = \frac{(M_h)_{\min}}{(M_h)_{\min,0}} - \sqrt{\frac{(M_h)_{\min,0}}{(M_h)_{\min}}}, \quad (171)$$

where we have introduced the appropriate length scale

$$a_* = \frac{2^{2/3}\sigma^{2/3}\alpha^{2/3}\nu^{1/3}}{6\pi\zeta} \left( \frac{Gm^5}{\hbar^2 \Sigma_0^2} \right)^{1/3}. \quad (172)$$

The prefactor is 0.553. Measuring the DM particle mass in units of  $10^{-22}\text{eV}/c^2$ , we get  $a_* = 1.28 \times 10^{-62} m^{5/3} \text{fm}$ . For  $a_s = 0$  we recover  $(M_h)_{\min} = (M_h)_{\min,0}$ . More generally, the noninteracting limit is valid for  $|a_s| \ll a_*$ . The relation  $(M_h)_{\min}/(M_h)_{\min,0}$  vs  $a_s/a_*$  is plotted in Fig. 8. For a given mass  $m$ , we see that  $(M_h)_{\min}$  is larger than  $(M_h)_{\min,0}$  when  $a_s > 0$  and smaller when  $a_s < 0$ .

(i) In the repulsive case, for  $a_s \gg a_*$ , we have

$$\frac{(M_h)_{\min}}{(M_h)_{\min,0}} \sim \frac{a_s}{a_*}. \quad (173)$$

This corresponds to the TF limit. Returning to the original variables, we obtain

$$(M_h)_{\min} \sim \frac{6\pi\zeta}{\alpha\nu} \frac{a_s \hbar^2 \Sigma_0}{Gm^3}. \quad (174)$$

The prefactor is 5.28. This can be compared with Eq. (43).

(ii) In the attractive case, for  $|a_s| \gg a_*$ , we have

$$\frac{(M_h)_{\min}}{(M_h)_{\min,0}} \sim \left( \frac{a_*}{a_s} \right)^2. \quad (175)$$

This corresponds to the nongravitational limit in which the configurations are unstable. Returning to the original variables, we obtain

$$(M_h)_{\min} \sim \frac{4\sigma^2\alpha}{(6\pi\zeta)^2} \frac{m^2}{\Sigma_0 a_s^2}. \quad (176)$$

The prefactor is 0.892. On the other hand, the normalized maximum mass (166) can be written as

$$\frac{(M_c)_{\max}}{(M_h)_{\min,0}} = \frac{1}{2} \left( \frac{a_*}{|a_s|} \right)^{1/2}. \quad (177)$$

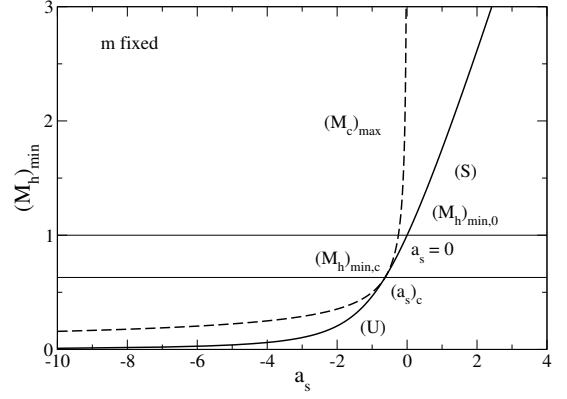


FIG. 8: Minimum halo mass  $(M_h)_{\min}$  as a function of the scattering length  $a_s$  for a fixed mass  $m$  of the DM particle (solid line). We have also plotted the maximum mass  $(M_c)_{\max}$  [6] as a function of  $a_s < 0$  (dashed line). The mass is normalized by  $(M_h)_{\min,0}$  and the scattering length by  $a_*$ . The stable part of the curve starts at the critical minimum halo point  $((a_s)_c, (M_h)_{\min,c})$ .

We find that the minimum halo is critical (i.e.  $(M_h)_{\min} = (M_c)_{\max}$ ) for

$$\frac{(a_s)_c}{a_*} = -\frac{1}{2^{2/3}}, \quad \frac{(M_h)_{\min,c}}{(M_h)_{\min,0}} = \frac{1}{2^{2/3}}. \quad (178)$$

Returning to the original variables, we obtain

$$(a_s)_c = -\frac{\sigma^{2/3}\alpha^{2/3}\nu^{1/3}}{6\pi\zeta} \left( \frac{Gm^5}{\hbar^2 \Sigma_0^2} \right)^{1/3}, \quad (179)$$

$$(M_h)_{\min,c} = \frac{\sigma^{2/3}}{\alpha^{1/3}\nu^{2/3}} \left( \frac{\hbar^4 \Sigma_0}{G^2 m^4} \right)^{1/3}. \quad (180)$$

The prefactors are 0.348 and 1.84. Measuring the DM particle mass in units of  $10^{-22}\text{eV}/c^2$ , we get  $(a_s)_c = -8.06 \times 10^{-63} m^{5/3} \text{fm}$  and  $(M_h)_{\min,c} = 1.86 \times 10^8 m^{-4/3} M_\odot$ . These relations can be directly obtained by writing  $\Sigma_0 = \alpha(M_c)_{\max}/(R_c)_*^2$  and using Eqs. (166) and (167). Stable minimum halos exist only for  $a_s \geq (a_s)_c$ . They have a mass  $(M_h)_{\min} \geq (M_h)_{\min,c}$ . When  $a_s < (a_s)_c$  the minimum halos are unstable (they correspond to the branch  $R_c < (R_c)_*$  of the mass-radius relation). We note that  $(M_h)_{\min,c}$  is relatively close to  $(M_h)_{\min,0}$ . Therefore, when  $(a_s)_c < a_s < 0$ , the minimum halo mass  $(M_h)_{\min}$  is always of the order of  $(M_h)_{\min,0}$  (see the stripe in Fig. 8).

For bosons with an attractive self-interaction, like the axion [11], it is more convenient to express the results in terms of the decay constant (see, e.g., [52])

$$f = \left( \frac{\hbar c^3 m}{32\pi |a_s|} \right)^{1/2}, \quad (181)$$

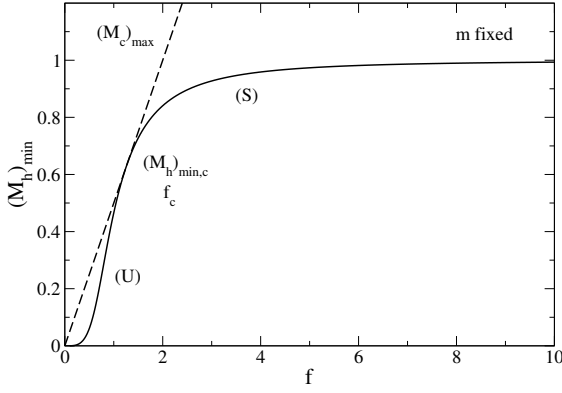


FIG. 9: Minimum halo mass  $(M_h)_{\min}$  as a function of the decay constant  $f$  for a fixed mass  $m$  of the DM particle (solid line). We have also plotted the maximum mass  $(M_c)_{\max}$  [6] as a function of  $f$  (dashed line). The mass is normalized by  $(M_h)_{\min,0}$  and the decay constant by  $f_*$ . The stable part of the curve starts at the critical minimum halo point  $(f_c, (M_h)_{\min,c})$ .

rather than the scattering length  $a_s$ . We can write

$$\frac{f}{f_*} = \left( \frac{a_*}{|a_s|} \right)^{1/2} \quad (182)$$

with

$$f_* = \frac{(6\pi\zeta)^{1/2}}{(32\pi)^{1/2} 2^{1/3} \sigma^{1/3} \alpha^{1/3} \nu^{1/6}} \frac{\hbar^{5/6} \Sigma_0^{1/3} c^{3/2}}{G^{1/6} m^{1/3}}. \quad (183)$$

The prefactor is 0.134. Measuring the DM particle mass in units of  $10^{-22} \text{eV}/c^2$ , we get  $f_* = 1.24 \times 10^{14} m^{-1/3} \text{GeV}$ . Eq. (171) can be rewritten as

$$\left( \frac{f_*}{f} \right)^2 = \sqrt{\frac{(M_h)_{\min,0}}{(M_h)_{\min}}} - \frac{(M_h)_{\min}}{(M_h)_{\min,0}}. \quad (184)$$

It determines the minimum halo mass  $(M_h)_{\min}$  in terms of  $m$  and  $f$ . This relation is plotted in Fig. 9. The maximum mass (166) can be written as

$$(M_c)_{\max} = \left( \frac{32\pi\sigma^2}{6\pi\zeta\nu} \right)^{1/2} \left( \frac{\hbar}{Gc^3} \right)^{1/2} \frac{f}{m} \quad (185)$$

or, in normalized form, as

$$\frac{(M_c)_{\max}}{(M_h)_{\min,0}} = \frac{1}{2} \frac{f}{f_*}. \quad (186)$$

Using Eqs. (178) and (182), the minimum decay constant corresponding to the critical minimum halo is

$$\frac{f_c}{f_*} = 2^{1/3}. \quad (187)$$

Returning to the original variables, we find

$$f_c = \frac{(6\pi\zeta)^{1/2}}{(32\pi)^{1/2} \sigma^{1/3} \alpha^{1/3} \nu^{1/6}} \frac{\hbar^{5/6} \Sigma_0^{1/3} c^{3/2}}{G^{1/6} m^{1/3}}. \quad (188)$$

The prefactor is 0.169. Measuring the DM particle mass in units of  $10^{-22} \text{eV}/c^2$ , we get  $f_c = 1.56 \times 10^{14} m^{-1/3} \text{GeV}$ . Only the upper part of the curve  $(M_h)_{\min}(f)$  starting from the point  $(f_c, (M_h)_{\min,c})$  is stable. The noninteracting limit corresponds to  $f \gg f_*$ .

### C. The $m(a_s)$ and $m(f)$ relations

If we consider that the minimum halo mass  $(M_h)_{\min}$  is known from the observations, and take  $(M_h)_{\min} \sim 10^8 M_\odot$  (Fornax) to fix the ideas, we can use the relation (171) to determine the mass  $m$  that the DM particle must have as a function of its scattering length  $a_s$  in order to match the value of the minimum halo mass  $(M_h)_{\min}$ . For  $a_s = 0$  we find from Eq. (170) that

$$m_0 = \frac{2^{1/2} \sigma^{1/2}}{\nu^{1/2} \alpha^{1/4}} \frac{\hbar \Sigma_0^{1/4}}{G^{1/2} (M_h)_{\min}^{3/4}}. \quad (189)$$

The prefactor is 2.23. In that case we obtain  $m_0 = 2.25 \times 10^{-22} \text{eV}/c^2$  which can be compared to Eq. (24). We can then write

$$\frac{(M_h)_{\min}}{(M_h)_{\min,0}} = \left( \frac{m}{m_0} \right)^{4/3}. \quad (190)$$

On the other hand, we can write

$$\frac{a_s}{a_*} = \frac{a_s}{a'_*} \left( \frac{m_0}{m} \right)^{5/3}, \quad (191)$$

where we have introduced the appropriate length scale

$$a'_* = \frac{2^{3/2} \sigma^{3/2} \alpha^{1/4}}{\nu^{1/2} 6\pi\zeta} \frac{\hbar}{G^{1/2} \Sigma_0^{1/4} (M_h)_{\min}^{5/4}}. \quad (192)$$

The prefactor is 2.11. We find  $a'_* = 4.95 \times 10^{-62} \text{fm}$ . Substituting Eqs. (190) and (191) into Eq. (171), we obtain

$$\frac{a_s}{a'_*} = \left( \frac{m}{m_0} \right)^3 - \frac{m}{m_0}. \quad (193)$$

This relation determines the mass  $m$  of the DM particle as a function of its scattering length  $a_s$  in order to yield a minimum halo of mass  $(M_h)_{\min}$ . It is plotted in Fig. 10. For  $a_s = 0$ , we recover  $m = m_0$ . More generally, the noninteracting limit corresponds to  $|a_s| \ll a_*$ . We see that  $m$  is larger than  $m_0$  when  $a_s > 0$  and smaller when  $a_s < 0$ . Therefore, we can increase the DM particle mass by allowing for a repulsive self-interaction between the bosons. As discussed in Appendix D.4 of [14] this could alleviate some tensions with observations of the Lyman- $\alpha$  forest encountered in the noninteracting model [27]. By contrast, an attractive self-interaction implies a (slightly) smaller DM particle mass and may therefore be even more in conflict with observations of the Lyman- $\alpha$

forest. As a result, a repulsive self-interaction ( $a_s > 0$ ) is privileged over an attractive self-interaction ( $a_s < 0$ ).

(i) In the repulsive case, for  $a_s \gg a'_*$ , we have

$$\frac{m}{m_0} \sim \left( \frac{a_s}{a'_*} \right)^{1/3}. \quad (194)$$

This corresponds to the TF limit. Returning to the original variables, we obtain

$$\frac{a_s}{m^3} \sim \frac{\nu\alpha}{6\pi\zeta} \frac{G(M_h)_{\min}}{\hbar^2 \Sigma_0}. \quad (195)$$

The prefactor is 0.189. We find  $a_s/m^3 = 4.35 \times 10^3 \text{ fm}/(\text{eV}/c^2)^3$  which can be compared with Eq. (39).

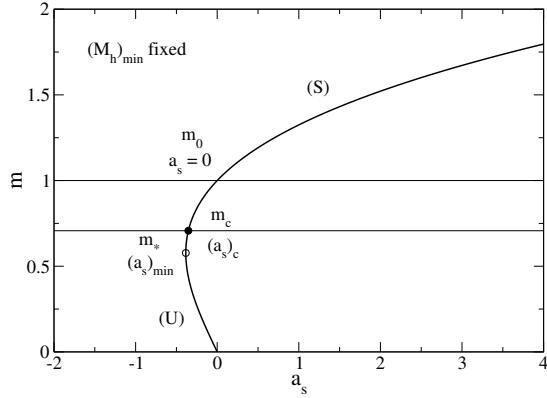


FIG. 10: Mass  $m$  of the DM particle as a function of its scattering length  $a_s$  for a fixed minimum halo mass  $(M_h)_{\min}$  (solid line). The mass is normalized by  $m_0$  and the scattering length by  $a'_*$ . The stable part of the curve starts at the critical minimum halo point  $((a_s)_c, m_c)$ .

(ii) In the attractive case, the curve  $m(a_s)$  presents a turning point at

$$\frac{(a_s)_{\min}}{a'_*} = -\frac{2}{3\sqrt{3}}, \quad \frac{m_*}{m_0} = \frac{1}{\sqrt{3}}. \quad (196)$$

However, this turning point does not correspond to the critical minimum halo for which [see Eqs. (178), (190) and (191)]

$$\frac{(a_s)_c}{a'_*} = -\frac{1}{2^{3/2}}, \quad \frac{m_c}{m_0} = \frac{1}{\sqrt{2}}. \quad (197)$$

Returning to the original variables, we find

$$(a_s)_c = -\frac{\sigma^{3/2} \alpha^{1/4}}{6\pi\zeta \nu^{1/2}} \frac{\hbar}{G^{1/2} \Sigma_0^{1/4} (M_h)_{\min}^{5/4}}, \quad (198)$$

$$m_c = \frac{\sigma^{1/2}}{\alpha^{1/4} \nu^{1/2}} \frac{\hbar \Sigma_0^{1/4}}{G^{1/2} (M_h)_{\min}^{3/4}}. \quad (199)$$

The prefactors are 0.746 and 1.58. We find  $(a_s)_c = -1.75 \times 10^{-62} \text{ fm}$  and  $m_c = 1.59 \times 10^{-22} \text{ eV}/c^2$  which

can be compared with Eq. (D19) in Appendix D of [14]. Only the upper part of the curve  $m(a_s)$  starting from the point  $((a_s)_c, m_c)$  is stable. The existence of stable minimum halos in the Universe implies that  $a_s \geq (a_s)_c$ . In that case, the DM particle mass satisfies  $m \geq m_c$ . We note that  $m_c$  is relatively close to  $m_0$ . Therefore, when  $(a_s)_c < a_s < 0$ , the minimum DM particle mass  $m$  is always of the order of  $m_0$  (see the stripe in Fig. 10).

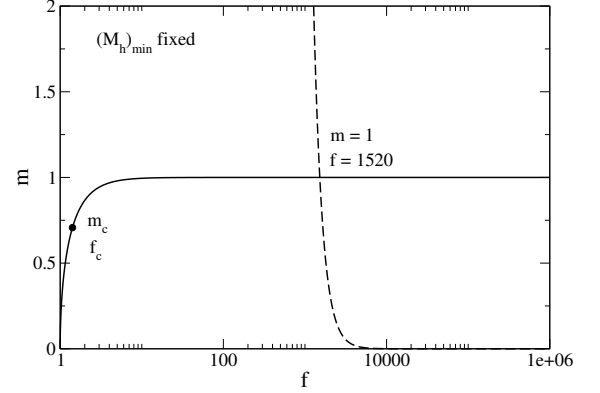


FIG. 11: Mass  $m$  of the DM particle as a function of its decay constant  $f$  for a fixed minimum halo mass  $(M_h)_{\min}$  (solid line). The mass is normalized by  $m_0$  and the decay constant by  $f'_*$ . The stable part of the curve starts at the critical minimum halo point  $(f_c, m_c)$ . The dashed line corresponds to Eq. (206) predicted by particle physics and cosmology. The intersection between the two curves determine the mass and the decay constant of the DM particle.

For bosons with an attractive self-interaction, like the axion [11], it is more convenient to express the results in terms of the decay constant (181). We can write

$$\frac{f}{f'_*} = \left( \frac{m}{m_0} \right)^{1/2} \left( \frac{a'_*}{|a_s|} \right)^{1/2} \quad (200)$$

with

$$f'_* = \frac{(6\pi\zeta)^{1/2}}{8\pi^{1/2} \sigma^{1/2} \alpha^{1/4}} \hbar^{1/2} \Sigma_0^{1/4} (M_h)_{\min}^{1/4} c^{3/2}. \quad (201)$$

The prefactor is 0.103. We find  $f'_* = 9.45 \times 10^{13} \text{ GeV}$ . Eq. (193) can be rewritten as

$$\frac{m}{m_0} = \sqrt{1 - \left( \frac{f'_*}{f} \right)^2}. \quad (202)$$

It determines the relation between  $m$  and  $f$  in order to have a minimum halo (ground state) of mass  $(M_h)_{\min}$ . This relation is plotted in Fig. 11. Using Eqs. (197) and (200), the minimum decay constant corresponding to the critical minimum halo is

$$\frac{f_c}{f'_*} = \sqrt{2}. \quad (203)$$

Returning to the original variables, we find

$$f_c = \frac{\sqrt{2}(6\pi\zeta)^{1/2}}{8\pi^{1/2}\sigma^{1/2}\alpha^{1/4}} \hbar^{1/2}\Sigma_0^{1/4}(M_h)_{\min}^{1/4} c^{3/2}. \quad (204)$$

The prefactor is 0.146. We find  $f_c = 1.34 \times 10^{14}$  GeV. Only the upper part of the curve  $m(f)$  starting from the point  $(f_c, m_c)$  is stable. The existence of stable minimum halos in the Universe implies that  $f \geq f_c$ . In that case, the DM particle mass satisfies  $m \geq m_c$ . The noninteracting limit corresponds to  $f \gg f'_*$ .

There is an interesting by-product of our analysis. Indeed, particle physics and cosmology lead to the following relation between  $f$  and  $m$  [27]:

$$\Omega_{\text{axion}} \sim 0.1 \left( \frac{f}{10^{17} \text{ GeV}} \right)^2 \left( \frac{m}{10^{-22} \text{ eV}} \right)^{1/2}. \quad (205)$$

Taking  $\Omega_{\text{axion}} \sim \Omega_{\text{m},0} = 0.3089$  and  $(M_h)_{\min} \sim 10^8 M_\odot$ , this relation can be rewritten as

$$\frac{m}{m_0} \sim 5.32 \times 10^{12} \left( \frac{f}{f'_*} \right)^{-4}. \quad (206)$$

This relation is independent from Eq. (202). Equating Eqs. (202) and (206), we obtain  $f = 1520 f'_* = 1.44 \times 10^{17}$  GeV and  $m = m_0 = 2.25 \times 10^{-22}$  eV/ $c^2$ . Therefore, we can determine  $f$  and  $m$  *individually*. We note that  $m$  has the same value as in the noninteracting case while  $f$  has a finite value  $f = 1520 f'_* = 1.44 \times 10^{17}$  GeV. It corresponds to  $a_s = -2.14 \times 10^{-68}$  fm. Interestingly,  $f$  lies in the range  $10^{16} \text{ GeV} \leq f \leq 10^{18} \text{ GeV}$  expected in particle physics [27] (we stress that the value of  $f$  has been *deduced* from our model based on the core mass-radius relation (162)). Since  $f \gg f'_*$ , we are essentially in the noninteracting regime.

*Remark:* we note that for the critical minimum halo the ratio

$$\frac{(a_s)_c}{m_c^{5/3}} = -\frac{\sigma^{2/3}\alpha^{2/3}\nu^{1/3}}{6\pi\zeta} \left( \frac{G}{\hbar^2\Sigma_0^2} \right)^{1/3} \quad (207)$$

is independent of  $(M_h)_{\min}$ . The prefactor is 0.348. We find  $(a_s)_c/m_c^{5/3} = -3.75 \times 10^{-26} \text{ fm}/(\text{eV}/c^2)^{5/3}$ .

#### D. The $M_c(M_h)$ relation

To obtain the core mass – halo mass relation  $M_c(M_h)$  we use the velocity dispersion tracing relation (121), the mass-radius relation (163) and the relation  $M_h = 1.76 \Sigma_0 r_h^2$  from Eq. (50). We obtain

$$\frac{M_c}{(M_h)_{\min,0}} = \left( \frac{M_h}{(M_h)_{\min,0}} \right)^{1/4} \sqrt{1 + \frac{a_s}{a_*} \left( \frac{M_h}{(M_h)_{\min,0}} \right)^{1/2}}. \quad (208)$$

For convenience, we have taken  $\alpha = 1/1.76$ . In this manner, when  $M_c = M_h$ , we recover the condition (171) determining the minimum halo mass.<sup>13</sup> For  $a_s = 0$ , we get

$$\frac{M_c}{(M_h)_{\min,0}} = \left( \frac{M_h}{(M_h)_{\min,0}} \right)^{1/4}. \quad (210)$$

This relation is also valid for  $|a_s| \ll a_*$ . We recover the scaling from Eq. (135). Returning to the original variables, we get

$$M_c = \frac{2^{1/2}\sigma^{1/2}}{\nu^{1/2}\alpha^{1/4}} \left( \frac{\hbar^4\Sigma_0 M_h}{G^2 m^4} \right)^{1/4}. \quad (211)$$

The prefactor is 2.23. For a DM halo of mass  $M_h = 10^{12} M_\odot$  similar to the one that surrounds our Galaxy, we obtain a core mass  $M_c = 10^9 M_\odot$  (we have taken  $(M_h)_{\min} = 10^8 M_\odot$ ).

(i) In the repulsive case, for  $a_s \gg a_*$  or  $M_h \gg M_{\min,0}$ , we have

$$\frac{M_c}{(M_h)_{\min,0}} = \left( \frac{a_s}{a_*} \right)^{1/2} \left( \frac{M_h}{(M_h)_{\min,0}} \right)^{1/2}. \quad (212)$$

This corresponds to the TF limit. Using Eq. (173), we obtain

$$\frac{M_c}{(M_h)_{\min}} = \left( \frac{M_h}{(M_h)_{\min}} \right)^{1/2}. \quad (213)$$

We recover the scaling from Eq. (145). Returning to the original variables, we get

$$M_c = \frac{(6\pi\zeta)^{1/2}}{\nu^{1/2}\alpha^{1/2}} \left( \frac{\hbar^2\Sigma_0 a_s M_h}{G m^3} \right)^{1/2}. \quad (214)$$

The prefactor is 2.30. For a DM halo of mass  $M_h = 10^{12} M_\odot$  similar to the one that surrounds our Galaxy, we obtain a core mass  $M_c = 10^{10} M_\odot$  (we have taken  $(M_h)_{\min} = 10^8 M_\odot$ ). The core mass – halo mass relation for  $a_s > 0$  is plotted in Figs. 12 and 13. These solutions are valid for  $M_h > (M_h)_{\min}$ .

(ii) In the attractive case, the core mass vanishes at

$$\frac{(M_h)_{\text{Max}}}{(M_h)_{\min,0}} = \left( \frac{a_*}{a_s} \right)^2. \quad (215)$$

<sup>13</sup> This can be understood as follows. Combining Eqs. (121) and (50) we get

$$\frac{M_c}{R_c} = \sqrt{1.76 \Sigma_0 M_h}. \quad (209)$$

This equation, that uses the relation  $M_h \sim 1.76 \Sigma_0 r_h^2$ , is valid only for sufficiently large halos. However, if we extrapolate this equation to the minimum halo for which  $M_h = M_c$ , we get  $M_c/R_c^2 = 1.76 \Sigma_0$ . Comparing this equation with Eq. (169) we obtain  $\alpha = 1/1.76$ .

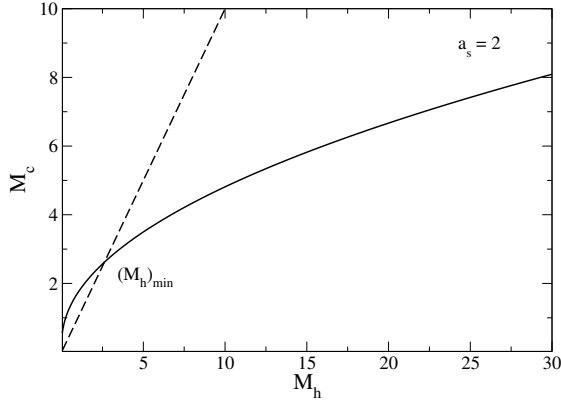


FIG. 12: Core mass  $M_c$  as a function of the halo mass  $M_h$  for a repulsive self-interaction  $a_s > 0$  (solid line). We have also plotted the relation  $M_c = M_h$  (dashed line) determining the minimum halo mass  $(M_h)_{\min}$ . The mass is normalized by  $(M_h)_{\min,0}$  and the scattering length by  $a_*$ .

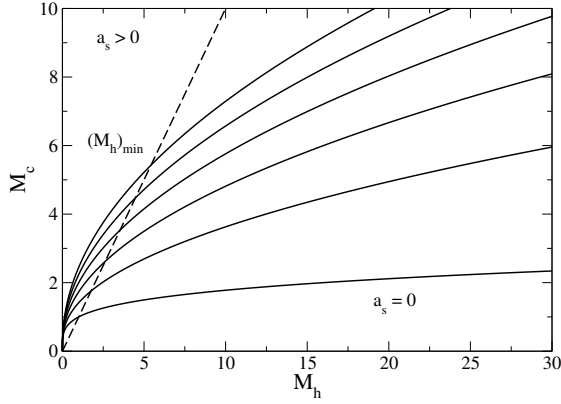


FIG. 13: Core mass  $M_c$  as a function of the halo mass  $M_h$  for different values of the scattering length  $a_s \geq 0$  and a fixed value of the mass  $m$  (solid lines). We have plotted the position of the minimum halo mass  $(M_h)_{\min}$  (dashed line). The mass is normalized by  $(M_h)_{\min,0}$ . We have indicated the curve corresponding to the noninteracting case  $a_s = 0$ .

On the other hand the core mass is maximum at

$$\frac{(M_h)_{\max}}{(M_h)_{\min,0}} = \frac{1}{4} \left( \frac{a_*}{a_s} \right)^2 \quad (216)$$

with the value

$$\frac{(M_c)_{\max}}{(M_h)_{\min,0}} = \frac{1}{2} \left( \frac{a_*}{|a_s|} \right)^{1/2}. \quad (217)$$

This corresponds to the maximum core mass given by Eq. (177). The core mass – halo mass relation for  $a_s < 0$  is plotted in Figs. 14 and 15. These solutions are valid for  $M_h > (M_h)_{\min}$ . On the other hand, the branch  $(M_h)_{\max} \leq M_h \leq (M_h)_{\max}$  corresponds to unstable states so that only the branch  $(M_h)_{\min} \leq$

$M_h \leq (M_h)_{\max}$ , corresponding to stable states, is physical. In summary, when  $a_s < (a_s)_c$  there is no halo with a stable quantum core (see Sec. VII B). When  $(a_s)_c < a_s < 0$  a stable quantum core exists only in the range  $(M_h)_{\min} \leq M_h \leq (M_h)_{\max}$ . It has a mass  $(M_h)_{\min} \leq M_c \leq (M_c)_{\max}$ . Coming back to the original variables, the maximum halo mass is

$$(M_h)_{\max} = \frac{\sigma^2 \alpha}{(6\pi\zeta)^2} \frac{m^2}{a_s^2 \Sigma_0}. \quad (218)$$

The prefactor is 0.223. Note that if we determine the maximum halo mass  $(M_h)_{\max}$  approximately by equating Eqs. (210) and (177) [or equivalently Eqs. (211) and (166)], we obtain a value that differs from the real one [Eq. (216) or equivalently (218)] by a factor 1/4.

For bosons with an attractive self-interaction, like the axion [11], it is more convenient to express the results in terms of the decay constant (181). When  $f < f_c$  there is no halo with a stable quantum core. When  $f > f_c$  a stable quantum core exists only in the range  $(M_h)_{\min} \leq M_h \leq (M_h)_{\max}$ . The minimum halo mass  $(M_h)_{\min}$  is close to  $(M_h)_{\min,0}$  given by Eq. (170). The maximum halo mass and the maximum core mass can be written as

$$(M_h)_{\max} = \frac{\sigma^2 \alpha (32\pi)^2}{(6\pi\zeta)^2} \frac{f^4}{\hbar^2 c^6 \Sigma_0}, \quad (219)$$

$$(M_c)_{\max} = \left( \frac{32\pi\sigma^2}{6\pi\zeta\nu} \right)^{1/2} \left( \frac{f^2 \hbar}{c^3 m^2 G} \right)^{1/2}. \quad (220)$$

We note that the maximum halo mass depends only on  $f$  while the maximum core mass depends on  $f$  and  $m$ . The prefactors are 2255 and 10.9. Measuring the DM particle mass in units of  $10^{-22} \text{eV}/c^2$  and the decay constant in units of  $10^{15} \text{GeV}$ , we get  $(M_h)_{\max} = 3.14 \times 10^{11} f^4 M_\odot$  and  $(M_c)_{\max} = 1.19 \times 10^9 (f/m) M_\odot$ . For  $f = 1.44 \times 10^{17} \text{GeV}$  and  $m = 2.25 \times 10^{-22} \text{eV}/c^2$  (see Sec. VII C), we get  $(M_h)_{\max} = 1.35 \times 10^{20} M_\odot$  and  $(M_c)_{\max} = 7.62 \times 10^{10} M_\odot$ . Since the largest DM halos observed in the Universe have a mass  $M_h \sim 10^{14} M_\odot \ll (M_h)_{\max}$ , these results suggest that the effect of an attractive self-interaction is negligible. This favors the consideration of a repulsive self-interaction [7].

In this section, we have expressed the core mass – halo mass relation in terms of  $M_h$ . This relation could easily be expressed in terms of  $M_v$  by using Eq. (132) with  $B \sim 2 \times 10^{-3}$ .

*Remark:* We can directly obtain the expression (218) of the maximum halo mass  $(M_h)_{\max}$  from the relation [see Eq. (209)]

$$\frac{(M_c)_{\max}}{(R_c)_*} = \sqrt{1.76 \Sigma_0 (M_h)_{\max}} \quad (221)$$

with Eqs. (166) and (167). If we consider a self-gravitating BEC with a central black hole it can be shown that the ratio  $(M_c)_{\max}/(R_c)_*$  is independent of the black hole mass. This implies that the expression (218) of the maximum halo mass is unchanged.

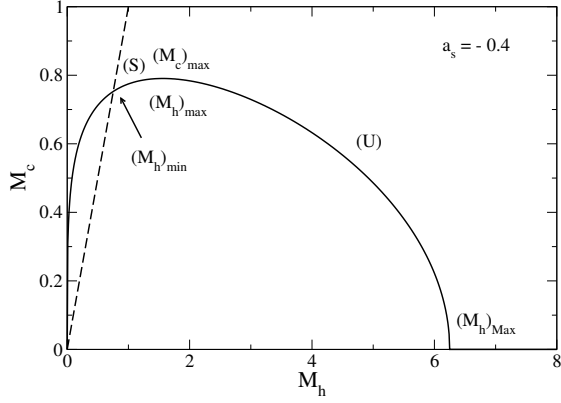


FIG. 14: Core mass  $M_c$  as a function of the halo mass  $M_h$  for an attractive self-interaction  $a_s < 0$  (solid line). We have also plotted the relation  $M_c = M_h$  (dashed line) determining the minimum halo mass  $(M_h)_{\min}$ . The mass is normalized by  $(M_h)_{\min,0}$  and the scattering length by  $a_*$ .

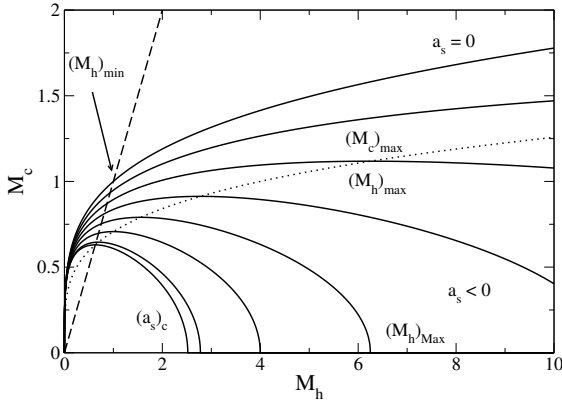


FIG. 15: Core mass  $M_c$  as a function of the halo mass  $M_h$  for different values of the scattering length  $a_s \leq 0$  and a fixed value of the mass  $m$  (solid lines). We have plotted the position of the minimum halo mass  $(M_h)_{\min}$  (dashed line) and the position of the maximum halo mass  $(M_h)_{\max}$  (dotted line). The mass is normalized by  $(M_h)_{\min,0}$ . We have indicated the curve corresponding to the minimum scattering length  $(a_s)_c$  for which  $(M_h)_{\min} = (M_h)_{\max}$  and the curve corresponding to the noninteracting case  $a_s = 0$ .

### E. Summary

In the noninteracting case ( $a_s = 0$ ) the halos with a mass  $M_h > (M_h)_{\min,0}$  [see Eq. (170)] contain a quantum core of mass  $M_c$  given by Eq. (210). All the configurations are stable.

For a repulsive self-interaction ( $a_s > 0$ ) the halos with a mass  $M_h > (M_h)_{\min}$  [see Eq. (171)] contain a quantum core of mass  $M_c$  given by Eq. (208). For  $a_s \ll a_*$  and  $M_h$  not too large, we are in the noninteracting limit discussed previously. For  $a_s \gg a_*$  or  $M_h$  sufficiently large  $(M_h/(M_h)_{\min} \gg (a_*/a_s)^2)$  we are in the TF limit. In

that case, the minimum halo mass  $(M_h)_{\min}$  is given by Eq. (174) and the mass  $M_c$  of the quantum core is given by Eq. (213). All the configurations are stable.

For an attractive self-interaction ( $a_s < 0$ ) the halos can contain a stable quantum core only if  $(a_s)_c < a_s < 0$  [see Eq. (179)] or equivalently if  $f > f_c$  [see Eq. (188)]. When this condition is fulfilled the quantum core is stable for  $(M_h)_{\min} < M_h < (M_h)_{\max}$ . The minimum halo mass  $(M_h)_{\min}$  [see Eqs. (171) and (184)] is of the order of  $(M_h)_{\min,0}$  [see Eq. (170)]. When we reach the maximum halo mass [see Eqs. (218) and (219)], the core reaches its maximum limit [see Eqs. (166) and (220)] and collapses. The result of the collapse (dense axion star, black hole, bosenova...) is discussed in [46–54].

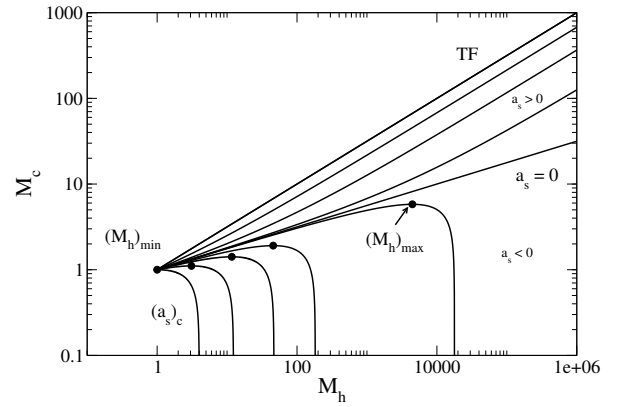


FIG. 16: Core mass  $M_c$  as a function of the halo mass  $M_h$  for different values of  $a_s/a_* = (a_s/a'_*)(m_0/m)^{5/3}$  with  $a_s/a'_* = (m/m_0)^3 - m/m_0$  [see Eqs. (191) and (193)] so that the minimum halo mass  $(M_h)_{\min}$  is fixed. The mass is normalized by  $(M_h)_{\min}$  (typically  $(M_h)_{\min} \sim 10^8 M_\odot$ ). These curves are obtained from Eqs. (171) and (208). We have plotted the position of the minimum halo mass  $(M_h)_{\min}$  (common origin) and the position of the maximum halo mass  $(M_h)_{\max}$  (bullets) when  $a_s < 0$ . We have indicated the curve corresponding to the minimum scattering length  $(a_s)_c/a_* = -1/2^{2/3}$  for which  $(M_h)_{\min} = (M_h)_{\max}$ , the curve corresponding to the noninteracting case  $a_s = 0$  [see Eq. (210)], and the curve corresponding to the TF limit  $a_s/a_* \gg 1$  [see Eq. (213)].

These results are summarized in Fig. 16 representing the general core mass – halo mass relation with a normalization such that the minimum halo mass is fixed whatever the values of  $m$  and  $a_s$ . Observations indicate that  $(M_h)_{\min} \sim 10^8 M_\odot$ . On this representation, we clearly see that the core mass increases more rapidly in the case of a repulsive self-interaction ( $a_s > 0$ ) than in the case of no interaction ( $a_s = 0$ ) or in the case of an attractive self-interaction ( $a_s < 0$ ). For  $a_s \geq 0$ , there is a stable core for any halo mass. For  $a_s < 0$ , there is a maximum halo mass associated with the existence of a maximum core mass.

### VIII. CONCLUSION

In this paper, we have analytically derived the core mass – halo mass relation of fermionic and bosonic DM halos from an effective thermodynamical approach. We have modeled the DM halos by a quantum core of mass  $M_c$  surrounded by an isothermal atmosphere of uniform density. We first determined an analytical expression of the free energy  $F(M_c)$  of the DM halos. The equilibrium core mass is then obtained by extremizing the free energy  $F(M_c)$  with respect to  $M_c$ . By representing the quantum core by a polytrope of index  $n$  we have developed a unified description for fermions ( $n = 3/2$ ), non-interacting bosons ( $n = 2$ ) and self-interacting bosons in the TF approximation ( $n = 1$ ). This allowed us to treat fermionic and bosonic DM halos with the same formalism. In the generic case, the extremization of the free energy  $F(M_c)$  determines three solutions corresponding to a gaseous phase (G), a core-halo phase (CH) and a condensed phase (C). The most important solution is the core-halo phase. We showed that this phase is unstable in the canonical ensemble but we argued (see also [7]) that it is probably stable in the microcanonical ensemble (the gaseous and condensed phase are stable in all the statistical ensembles).

Our thermodynamical approach leads to the velocity dispersion tracing relation (121) put forward in [7, 34]. Therefore, this relation can be justified by an effective thermodynamical approach. For noninteracting bosons, we obtain the mass-radius relation (138) which is consistent to the one found by Schive *et al.* [26]. For fermions, we obtain the mass-radius relation (157) which is consistent to the one found by Ruffini *et al.* [64]. For bosons with an attractive self-interaction in the TF limit, we predict the mass-radius relation (148) which still has to be confirmed numerically. Combining the velocity dispersion tracing relation [7, 34] with the core mass – core radius relation obtained in [6] we have obtained an approximate general core mass – halo mass relation  $M_c(M_v)$  [see Eq. (208)] that is valid for bosons with arbitrary repulsive or attractive self-interaction. For an attractive self-interaction, corresponding to axions [11], we have determined the maximum halo mass  $(M_v)_{\max}$  [see Eq. (219)] that can harbor a stable quantum core (dilute axion star).

Finally, we have argued that the mass scale of non-interacting DM bosons is determined in terms of fundamental constants by  $m_\Lambda = \hbar\sqrt{\Lambda}/c^2 = 2.08 \times 10^{-33} \text{ eV}/c^2$  while the mass scale of fermions is determined by  $m_\Lambda^* = (\Lambda\hbar^3/Gc^3)^{1/4} = \sqrt{m_\Lambda M_P} = 5.04 \times 10^{-3} \text{ eV}/c^2$ . We found that the prefactor between the actual DM particle mass and these fundamental mass scales can be very large (11 orders of magnitude for bosons and 4 orders of magnitude for fermions). However, these fundamental mass scales can explain the intrinsic difference of mass between bosonic and fermionic DM particles. Their ratio is  $m_\Lambda^*/m_\Lambda = (c^5/G\hbar\Lambda)^{1/4} = 2.42 \times 10^{30}$ , corresponding to a difference of 30 orders of magnitude.

Finally, in the case of self-interacting bosons, we have found that the fundamental scale of the ratio  $a_s/m^3$  is  $r_\Lambda/m_\Lambda^3 = 2Gc^2/\Lambda\hbar^2 = 6.11 \times 10^{17} \text{ fm}(\text{eV}/c^2)^{-3}$ .

In the present paper, we have developed an analytical model in which the isothermal atmosphere has a uniform density. This approximation is sufficient to obtain the correct scaling of the core mass – halo mass relation. However, in order to develop more accurate models of fermionic and bosonic DM halos, and in particular to be able to determine their density and circular velocity profiles, we need to solve a generalized Emden equation numerically. The case of self-gravitating BECs with a repulsive self-interaction has been treated in detail in [7]. The case of noninteracting bosons and fermions can be treated with the same method. These models are being presently investigated [65].

It will be important in future works to determine if DM is made of fermions or bosons (either noninteracting, with a repulsive self-interaction, or with an attractive self-interaction). All these models are very interesting from a physical point of view, with a lot of nice properties, but it is possible that some of them will be ruled out by observations. Alternatively, all these models could be of interest if DM is made of several types of particles (bosons and fermions) as suggested in [7].

### Appendix A: Polytopic spheres

In this Appendix, we recall general results of self-gravitating polytopic spheres [35, 66]. We apply them to the quantum models of DM halos at  $T = 0$  (ground states) discussed in Sec. II.

For classical self-gravitating systems, or for quantum self-gravitating systems in the TF approximation, the condition of hydrostatic equilibrium

$$\nabla P + \rho \nabla \Phi = \mathbf{0} \quad (\text{A1})$$

combined with the Poisson equation

$$\Delta \Phi = 4\pi G \rho \quad (\text{A2})$$

leads to the fundamental differential equation

$$\nabla \cdot \left( \frac{\nabla P}{\rho} \right) = -4\pi G \rho. \quad (\text{A3})$$

For a polytopic equation of state of the form

$$P = K \rho^\gamma, \quad (\text{A4})$$

where  $K$  is the polytopic constant and  $\gamma = 1 + 1/n$  is the polytopic index, the differential equation (A3) becomes

$$K(n+1)\Delta\rho^{1/n} = -4\pi G\rho. \quad (\text{A5})$$

In the following, we restrict ourselves to spherically symmetric distributions. We also assume  $K > 0$  and  $6/5 <$



$\gamma < +\infty$  (i.e.  $0 \leq n < 5$ ) for reasons explained below. With the substitution

$$\rho = \rho_0 \theta^n, \quad \xi = \frac{r}{r_0}, \quad (\text{A6})$$

where  $\rho_0$  is the central density and

$$r_0 = \left[ \frac{K(n+1)}{4\pi G \rho_0^{1-1/n}} \right]^{1/2} \quad (\text{A7})$$

is the polytropic radius, we obtain the Lane-Emden equation

$$\frac{1}{\xi^2} \frac{d}{d\xi} \left( \xi^2 \frac{d\theta}{d\xi} \right) = -\theta^n \quad (\text{A8})$$

with the boundary conditions

$$\theta(0) = 1, \quad \theta'(0) = 0. \quad (\text{A9})$$

According to the general results of Refs. [35, 66], a polytrope of index  $n$  has a compact support provided that  $0 \leq n < 5$ . In that case, the density falls off to zero at a finite radius. This characterizes a complete polytrope.<sup>14</sup> It is customary to denote by  $\xi_1$  the normalized radius at which the density vanishes:  $\theta_1 = 0$ . The radius and the mass of a complete polytrope are

$$R = \xi_1 \left[ \frac{K(n+1)}{4\pi G} \right]^{1/2} \frac{1}{\rho_0^{(n-1)/2n}}, \quad (\text{A10})$$

$$M = -4\pi \frac{\theta'_1}{\xi_1} \rho_0 R^3. \quad (\text{A11})$$

Eliminating  $\rho_0$  between these two relations, we find that the mass-radius relation of a complete polytrope of index  $n$  is

$$M^{(n-1)/n} R^{(3-n)/n} = \frac{K(1+n)}{G(4\pi)^{1/n}} \omega_n^{(n-1)/n}, \quad (\text{A12})$$

where  $\omega_n = -\xi_1^{(n+1)/(n-1)} \theta'_1$  is a constant determined by the Lane-Emden equation (A8). A complete polytrope of index  $n$  is dynamically stable with respect to the Euler-Poisson equations if  $n < 3$  and linearly unstable if  $n > 3$ .

For the polytrope  $n = 3/2$  (fermion stars), using Eq. (4), we find

$$\xi_1 = 3.65375, \quad \theta'_1 = -0.203302, \quad (\text{A13})$$

$$R = 0.35885 \frac{h}{m^{4/3} G^{1/2} \rho_0^{1/6}}, \quad (\text{A14})$$

<sup>14</sup> Polytropes with  $n > 5$  have an infinite mass. The polytrope  $n = 5$  is unbounded and has a finite mass. For this index, the Lane-Emden equation has a simple analytical expression discovered by Schuster [67]. It was used by Plummer [68] to fit the density profile of globular clusters (Plummer model).

$$M = 0.699218 \rho_0 R^3, \quad (\text{A15})$$

$$MR^3 = 0.0014931 \frac{h^6}{G^3 m^8}. \quad (\text{A16})$$

For the polytrope  $n = 2$  (noninteracting boson stars), using Eq. (E3), we find

$$\xi_1 = 4.353, \quad \theta'_1 = -0.1272, \quad (\text{A17})$$

$$R = 1.94415 \frac{h^{1/2}}{m^{1/2} G^{1/4} \rho_0^{1/4}}, \quad (\text{A18})$$

$$M = 0.367205 \rho_0 R^3, \quad (\text{A19})$$

$$MR = 5.24594 \frac{h^2}{G m^2}. \quad (\text{A20})$$

For the polytrope  $n = 1$  (self-interacting boson stars), using Eq. (30), we find

$$\xi_1 = \pi, \quad \theta'_1 = -1/\pi, \quad (\text{A21})$$

$$R = \pi \left( \frac{a_s h^2}{G m^3} \right)^{1/2} \quad (\text{A22})$$

$$M = \frac{4}{\pi} \rho_0 R^3, \quad (\text{A23})$$

## Appendix B: Total energy, eigenenergy and virial theorem of a self-gravitating BEC

We consider a self-gravitating BEC described by the GPP equations with a self-interaction corresponding to a power-law potential [55]. In the hydrodynamic representation of the GPP equations, a power-law potential of interaction gives rise to a polytropic equation of state. In that case, the total energy of the BEC is given by

$$E_{\text{tot}} = \Theta_Q + U + W. \quad (\text{B1})$$

This is the sum of the quantum kinetic energy

$$\Theta_Q = \frac{\hbar^2}{8m^2} \int \frac{(\nabla \rho)^2}{\rho} d\mathbf{r} = \frac{\hbar^2}{2m^2} \int (\nabla \sqrt{\rho})^2 d\mathbf{r}, \quad (\text{B2})$$

the internal energy

$$U = \frac{1}{\gamma - 1} \int P d\mathbf{r} = \frac{K}{\gamma - 1} \int \rho^\gamma d\mathbf{r}, \quad (\text{B3})$$

and the gravitational energy

$$W = \frac{1}{2} \int \rho \Phi d\mathbf{r}. \quad (\text{B4})$$

The eigenenergy  $E$  satisfies the relation

$$NE = \Theta_Q + \gamma U + 2W. \quad (\text{B5})$$

On the other hand, the equilibrium scalar virial theorem writes

$$2\Theta_Q + 3(\gamma - 1)U + W = 0. \quad (\text{B6})$$

For classical self-gravitating systems, or for self-gravitating BECs in the TF approximation where the quantum potential can be neglected, the foregoing equations reduce to

$$E_{\text{tot}} = U + W, \quad (\text{B7})$$

$$NE = \gamma U + 2W, \quad (\text{B8})$$

$$3(\gamma - 1)U + W = 0. \quad (\text{B9})$$

From these equations, we obtain the relations

$$E_{\text{tot}} = -\frac{3-n}{n}U = \frac{3-n}{3}W = \frac{3-n}{5-n}NE. \quad (\text{B10})$$

#### Appendix C: Betti-Ritter formula

For classical self-gravitating systems, or for self-gravitating BECs in the TF approximation, the condition of hydrostatic equilibrium is given by Eq. (A1). For a polytropic equation of state (A4) we have

$$\frac{\nabla P}{\rho} = (n+1)\nabla\left(\frac{P}{\rho}\right). \quad (\text{C1})$$

As a result, the condition of hydrostatic equilibrium (A1) can be integrated into

$$(n+1)\frac{P}{\rho} + \Phi = \frac{E}{m}, \quad (\text{C2})$$

where  $E$  is a constant of integration. For a self-gravitating BEC it represents the eigenenergy [55]. Multiplying Eq. (C2) by  $\rho$  and integrating over the whole configuration, we obtain Eq. (B8). Assuming  $6/5 < \gamma < +\infty$  (i.e.  $0 \leq n < 5$ ) so that  $P/\rho = 0$  on the boundary of the system  $r = R$  where the density vanishes, we find from Eq. (C2) that

$$\frac{E}{m} = \Phi(R) = -\frac{GM}{R}. \quad (\text{C3})$$

This equation determines the eigenenergy  $E$ . As a result, Eq. (B8) can be rewritten as

$$-\frac{GM^2}{R} = \gamma U + 2W. \quad (\text{C4})$$

Combining this relation with the equilibrium scalar virial theorem (B9) we obtain the Betti-Ritter formula

$$W = -\frac{3}{5-n}\frac{GM^2}{R} \quad (\text{C5})$$

determining the gravitational energy  $W$  of a polytropic sphere [35]. From Eqs. (C5) and (B10), we get

$$U = \frac{n}{5-n}\frac{GM^2}{R} \quad (\text{C6})$$

and

$$E_{\text{tot}} = -\frac{3-n}{5-n}\frac{GM^2}{R}. \quad (\text{C7})$$

From the last relation, we can directly conclude that complete polytropes with index  $n < 3$ , i.e.  $\gamma > 4/3$ , are stable (because  $E_{\text{tot}} < 0$ ) while complete polytropes with index  $n > 3$ , i.e.  $\gamma < 4/3$ , are unstable (because  $E_{\text{tot}} > 0$ ) [35].

#### Appendix D: Ledoux formula

The complex pulsation of a polytrope of index  $0 < n < 5$  is approximately given by the Ledoux formula [69]:<sup>15</sup>

$$\omega^2 = (4 - 3\gamma)\frac{W}{I}, \quad (\text{D1})$$

where  $I = \int \rho r^2 d\mathbf{r}$  is the moment of inertia of the system. Using the results of Appendix A it can be written as

$$I = \kappa_n MR^2 \quad \text{with} \quad \kappa_n = \frac{\int_0^{\xi_1} \theta^n \xi^4 d\xi}{\xi_1^2 \int_0^{\xi_1} \theta^n \xi^2 d\xi}. \quad (\text{D2})$$

Combining this equation with the Betti-Ritter formula (C5), we can rewrite Eq. (D1) as

$$\omega^2 = -\frac{3(n-3)}{(5-n)n\kappa_n}\frac{GM}{R^3}. \quad (\text{D3})$$

#### Appendix E: Density profile of a noninteracting self-gravitating BEC with a compact support: polytrope $n = 2$

The fundamental differential equation of quantum hydrostatic equilibrium determining the density profile of a noninteracting self-gravitating BEC is given by Eq. (17). On the other hand, the fundamental differential equation of classical hydrostatic equilibrium determining the density profile of a polytrope of index  $n$  is given by Eq. (A5). For  $n = 2$  it becomes

$$3K\Delta\sqrt{\rho} = -4\pi G\rho. \quad (\text{E1})$$

<sup>15</sup> This formula can also be obtained from a variational principle based on a Gaussian ansatz [55].

Dividing Eq. (E1) by  $\sqrt{\rho}$ , applying the Laplacian operator, and using Eq. (E1) again, we obtain

$$\Delta \left( \frac{\Delta \sqrt{\rho}}{\sqrt{\rho}} \right) = \left( \frac{4\pi G}{3K} \right)^2 \rho. \quad (\text{E2})$$

Remarkably, this equation coincides with Eq. (17) provided that we make the identification

$$K = \left( \frac{2\pi G \hbar^2}{9m^2} \right)^{1/2}. \quad (\text{E3})$$

As a result, the density profile of a polytrope of index  $n = 2$  and polytropic constant given by Eq. (E3) is a particular solution of Eq. (17).<sup>16</sup> Using the variables defined in Appendix A, it can be written as

$$\rho(r) = \rho_0 \theta(\xi)^2, \quad \xi = r/r_0, \quad r_0 = \left( \frac{\hbar^2}{8\pi G m^2 \rho_0} \right)^{1/4}, \quad (\text{E4})$$

where  $\theta(\xi)$  is the solution of the Lane-Emden equation (A8) of index  $n = 2$ .

A polytrope of index  $n = 2$  has a compact support and is stable. Furthermore, according to Eq. (A12), the mass-radius relation is

$$MR = \frac{1}{2} \omega_2 \frac{\hbar^2}{Gm^2} = 5.25 \frac{\hbar^2}{Gm^2}, \quad (\text{E5})$$

where we have used  $\omega_2 = 10.4950\dots$  Eq. (E5) displays the same scaling as the mass-radius relation from Eq. (18) but the prefactor is different. This is because the density profile given by Eq. (E4) is different from the density profile of the soliton that has been reported previously in the literature [17, 18, 21, 25–27, 37–39] (see Sec. II B). Indeed, the authors of Refs. [17, 18, 21, 25–27, 37–39] have looked for a solution of Eq. (17) corresponding to a density profile that goes to zero at infinity. Actually, there exists another solution of Eq. (17), given by Eq. (E4), corresponding to a density profile with a compact support that vanishes at a finite radius  $R$ .<sup>17</sup> Apparently, the two profiles are stable (they are plotted in Fig. 2). It may therefore be useful to compare their respective energy in order to determine which profile has the smallest energy (ground state).

The quantum kinetic of a BEC is given by Eq. (B2). Integrating the second expression by parts, we obtain

$$\Theta_Q = \frac{\hbar^2}{4m^2} \oint \nabla \rho \cdot d\mathbf{S} - \frac{\hbar^2}{2m^2} \int \sqrt{\rho} \Delta \sqrt{\rho} d\mathbf{r}. \quad (\text{E6})$$

Since  $\rho'(R) \propto \theta_1 \theta_1'$  for a polytrope of index  $n = 2$  [see Eq. (E4)] and since  $\theta_1 = 0$  and  $|\theta_1'| < +\infty$  (see Appendix A), we have  $\rho'(R) = 0$ . As a result, the surface term vanishes and Eq. (E6) reduces to

$$\Theta_Q = -\frac{\hbar^2}{2m^2} \int \sqrt{\rho} \Delta \sqrt{\rho} d\mathbf{r}. \quad (\text{E7})$$

Using Eq. (E1) we then find that

$$\Theta_Q = 3K \int \rho^{3/2} d\mathbf{r}. \quad (\text{E8})$$

This result can be compared to the internal energy (B3) of a polytrope of index  $n = 2$  which is

$$U = 2K \int \rho^{3/2} d\mathbf{r}. \quad (\text{E9})$$

We have the relation

$$\Theta_Q = \frac{3}{2} U. \quad (\text{E10})$$

Therefore, the energy  $E_{\text{tot}} = \Theta_Q + W$  of a self-gravitating noninteracting BEC with the density profile (E4) is different from the energy  $E_{\text{tot}} = U + W$  of the corresponding polytrope.

For a self-gravitating noninteracting BEC, we have (see Sec. II B)

$$E_{\text{tot}} = -\Theta_Q = \frac{1}{2} W. \quad (\text{E11})$$

On the other hand, the gravitational energy of a polytrope  $n = 2$  is (see Appendix C)

$$W = -\frac{GM^2}{R}. \quad (\text{E12})$$

Combining Eqs. (E11) and (E12) and using the mass-radius relation from Eq. (E5), we find that the energy of a self-gravitating noninteracting BEC with the density profile (E4) is

$$E_{\text{tot}} = -\frac{GM^2}{2R} = -\frac{1}{\omega_2} \frac{G^2 M^3 m^2}{\hbar^2} = -0.0953 \frac{G^2 M^3 m^2}{\hbar^2}. \quad (\text{E13})$$

This energy is smaller than the one given by Eq. (22). Therefore, the solution of Eq. (17) that has a compact support [see Eq. (E4)] has a smaller energy than the solution of Eq. (17) that extends to infinity (see Sec. II B). The ground state of the self-gravitating noninteracting BEC corresponds therefore to the solution considered in this Appendix, not to the solution that has been considered in Refs. [17, 18, 21, 25–27, 37–39] (see Sec. II B). However, in the case of systems with long-range interactions, we know that a metastable state (i.e. a local but not a global energy minimum) may have a very long lifetime and can be fully relevant. This may be the case of the solution considered in Refs. [17, 18, 21, 25–27, 37–39] which seems to be selected in direct numerical simulations [25, 26].

<sup>16</sup> We note that Eq. (E1) implies Eq. (E2) but the converse is wrong. As a result Eqs. (17) and (E1) are not equivalent.

<sup>17</sup> In Ref. [38] we found a solution of Eq. (17) for which “the program breaks down because the density achieves too small values ( $< 10^{-11}$ ).” This solution corresponds to the density profile (E4) with a compact support.

*Remark:* the energy of a polytrope of index  $n = 2$  can be obtained from the relations (see Appendices B and C):

$$E_{\text{tot}} = U + W, \quad (\text{E14})$$

$$NE = \frac{3}{2}U + 2W, \quad (\text{E15})$$

$$\frac{3}{2}U + W = 0, \quad (\text{E16})$$

implying

$$E_{\text{tot}} = -\frac{1}{2}U = \frac{1}{3}W = -\frac{GM^2}{3R}. \quad (\text{E17})$$

It differs from Eq. (E13) by a factor  $2/3$ .

## Appendix F: Gravitational energy

The gravitational energy of a spherically symmetric system is given by (see, e.g., Appendix G of [55])

$$W = - \int_0^{+\infty} \rho(r) \frac{GM(r)}{r} 4\pi r^2 dr, \quad (\text{F1})$$

where

$$M(r) = \int_0^r \rho(r) 4\pi r^2 dr \quad (\text{F2})$$

is the mass contained within the sphere of radius  $r$ . In our model, the system is made of a core of mass  $M_c$  and radius  $R_c$  and a uniform atmosphere of density  $\rho_a$  and mass  $M_a = M - M_c$  contained within the spheres of radius  $R_c$  and  $R$ . Therefore, we can write

$$W = W_c - 4\pi G \rho_a \int_{R_c}^R M(r) r dr, \quad (\text{F3})$$

where the first term  $W_c$  is the gravitational energy of the core and the second term  $W_a$  is the gravitational energy of the atmosphere in the presence of the core. For  $r \geq R_c$ , we have

$$M(r) = M_c + \frac{4}{3}\pi \rho_a (r^3 - R_c^3). \quad (\text{F4})$$

Substituting Eq. (F4) into Eq. (F3) and evaluating the integral we get

$$W = W_c - 4\pi G \rho_a \left[ M_c \frac{r^2}{2} + \frac{4}{15}\pi \rho_a r^5 - \frac{2}{3}\pi \rho_a R_c^3 r^2 \right]_{R_c}^R \quad (\text{F5})$$

with

$$\rho_a = \frac{3(M - M_c)}{4\pi(R^3 - R_c^3)}. \quad (\text{F6})$$

These expressions are exact. For our problem, it is a good approximation to assume that  $R \gg R_c$ . As a result, the foregoing equation simplifies into

$$W = W_c - 4\pi G \rho_a \left( M_c \frac{R^2}{2} + \frac{4}{15}\pi \rho_a R^5 \right) \quad (\text{F7})$$

with

$$\rho_a = \frac{3(M - M_c)}{4\pi R^3}. \quad (\text{F8})$$

We finally obtain

$$W = W_c - \frac{3GM_c(M - M_c)}{2R} - \frac{3G(M - M_c)^2}{5R}. \quad (\text{F9})$$

The first term is the potential energy of the core, the third term is the potential energy of the atmosphere and the second term is the interaction energy. This is as if we had a point mass  $M_c$  at  $r = 0$  [65].

## Appendix G: The minimum halo radius, the minimum halo mass and the maximum halo central density

In this Appendix, we determine the radius, the mass and the central density of the “minimum halo” assuming that it corresponds to the ground state ( $T = 0$ ) of a self-gravitating quantum gas. We have seen in Sec. II that it can be represented by a polytropic sphere. For the sake of generality we treat the case of an arbitrary polytropic index  $n$ , then consider particular cases corresponding to fermions, noninteracting bosons and self-interacting bosons in the TF limit.

### 1. General results

The halo radius  $r_h$  is defined as the distance at which the central density  $\rho_0$  is divided by 4. Using Eqs. (A6) and (A7), it is given by

$$r_h = \xi_h \left[ \frac{K(n+1)}{4\pi G} \right]^{1/2} \frac{1}{\rho_0^{(n-1)/2n}}, \quad (\text{G1})$$

where  $\xi_h$  is determined by the equation

$$\theta(\xi_h)^n = \frac{1}{4}. \quad (\text{G2})$$

The value of  $\xi_h$  can be obtained by solving the Lane-Emden equation (A8). The halo mass, which is the mass contained within the sphere of radius  $r_h$ , is given by

$$M_h = -4\pi \frac{\theta'(\xi_h)}{\xi_h} \rho_0 r_h^3. \quad (\text{G3})$$

Eliminating the central density between Eqs. (G1) and (G3), we obtain the halo mass-radius relation

$$M_h r_h^{(3-n)/(n-1)} = -4\pi\theta'(\xi_h)\xi_h^{(n+1)/(n-1)} \times \left[ \frac{K(n+1)}{4\pi G} \right]^{n/(n-1)}, \quad (\text{G4})$$

which is analogous to the mass-radius relation (A12). On the other hand, using Eqs. (G1) and (G3) and introducing the universal surface density of DM halos (1) we find that the minimum halo radius, the minimum halo mass, and the maximum halo central density are given by

$$(r_h)_{\min} = \xi_h^{2n/(n+1)} \left[ \frac{K(n+1)}{4\pi G} \right]^{n/(n+1)} \frac{1}{\Sigma_0^{(n-1)/(n+1)}} \quad (\text{G5})$$

and

$$(M_h)_{\min} = -4\pi\theta'(\xi_h)\xi_h^{(3n-1)/(n+1)} \times \left[ \frac{K(n+1)}{4\pi G} \right]^{2n/(n+1)} \Sigma_0^{(3-n)/(n+1)}. \quad (\text{G6})$$

$$(\rho_0)_{\max} = \frac{1}{\xi_h^{2n/(n+1)}} \left[ \frac{4\pi G}{K(n+1)} \right]^{n/(n+1)} \Sigma_0^{2n/(n+1)}. \quad (\text{G7})$$

### 2. Fermions

For the polytrope  $n = 3/2$  (fermion stars) using Eq. (4), we have

$$\xi_h = 2.27, \quad \theta'_h = -0.360. \quad (\text{G8})$$

$$r_h = 0.223 \frac{h}{m^{4/3} G^{1/2} \rho_0^{1/6}}, \quad (\text{G9})$$

$$M_h = 1.99 \rho_0 r_h^3, \quad (\text{G10})$$

$$M_h r_h^3 = 2.45 \times 10^{-4} \frac{h^6}{G^3 m^8}. \quad (\text{G11})$$

Using Eq. (1), we obtain Eqs. (13)-(15).

### 3. Noninteracting bosons

For the polytrope  $n = 2$  (noninteracting boson stars) we have

$$\xi_h = 2.092, \quad \theta'_h = -0.3216. \quad (\text{G12})$$

$$r_h = 0.934333 \frac{h^{1/2}}{m^{1/2} G^{1/4} \rho_0^{1/4}}, \quad (\text{G13})$$

$$M_h = 1.93181 \rho_0 r_h^3, \quad (\text{G14})$$

$$M_h r_h = 1.47221 \frac{h^2}{G m^2}. \quad (\text{G15})$$

Using Eq. (1), we obtain Eqs. (25)-(27).

### 4. Self-interacting bosons in the TF limit

For the polytrope  $n = 1$  (self-interacting boson stars) we have

$$\xi_h = 2.4746, \quad \theta'_h = -0.41853. \quad (\text{G16})$$

$$r_h = 2.4746 \left( \frac{a_s h^2}{G m^3} \right)^{1/2} \quad (\text{G17})$$

$$M_h = 2.12535 \rho_0 r_h^3, \quad (\text{G18})$$

Using Eq. (1), we obtain Eqs. (42)-(44).

## Appendix H: Results of the quantum Jeans instability theory

In this Appendix, we recapitulate the main results of the quantum Jeans instability theory developed in Refs. [6, 70], restricting ourselves to the nonrelativistic regime. We refer to these papers for details about their derivation and for some generalizations.

### 1. Fermions

If DM is made of fermions, the Jeans length and the Jeans mass are given by

$$\lambda_J = \frac{1}{2} \left( \frac{\pi}{3} \right)^{1/6} \frac{h}{G^{1/2} m^{4/3} \rho^{1/6}}, \quad (\text{H1})$$

$$M_J = \frac{4}{3} \pi \rho \left( \frac{\lambda_J}{2} \right)^3 = \frac{1}{16} \left( \frac{\pi}{3} \right)^{3/2} \frac{h^3 \rho^{1/2}}{G^{3/2} m^4}. \quad (\text{H2})$$

Eliminating the density between these expressions, we get the Jeans mass-radius relation

$$M_J \lambda_J^3 = \frac{\pi^2}{1152} \frac{h^6}{G^3 m^8}. \quad (\text{H3})$$

We can also define a Jeans surface density

$$\Sigma_J = \rho \frac{\lambda_J}{2} = \frac{1}{4} \left( \frac{\pi}{3} \right)^{1/6} \frac{h \rho^{5/6}}{G^{1/2} m^{4/3}}. \quad (\text{H4})$$

These equations display the same scalings as Eqs. (G9)-(G11) and (15) for DM halos.

## 2. Noninteracting bosons

If DM is made of noninteracting bosons, the Jeans length and the Jeans mass are given by

$$\lambda_J = 2\pi \left( \frac{\hbar^2}{16\pi G \rho m^2} \right)^{1/4}, \quad (\text{H5})$$

$$M_J = \frac{4}{3}\pi\rho \left( \frac{\lambda_J}{2} \right)^3 = \frac{\pi}{6} \left( \frac{\pi^3 \hbar^2 \rho^{1/3}}{G m^2} \right)^{3/4}. \quad (\text{H6})$$

Eliminating the density between these expressions, we get the Jeans mass-radius relation

$$M_J \lambda_J = \frac{\pi^4}{6} \frac{\hbar^2}{G m^2}. \quad (\text{H7})$$

The Jeans surface density is

$$\Sigma_J = \rho \frac{\lambda_J}{2} = \pi \left( \frac{\hbar^2 \rho^3}{16\pi G m^2} \right)^{1/4}. \quad (\text{H8})$$

These equations display the same scalings as Eqs. (G13)-(G15) and (27) for DM halos.

## 3. Self-interacting bosons in the TF limit

If DM is made of self-interacting bosons in the TF limit, the Jeans length and the Jeans mass are given by

$$\lambda_J = 2\pi \left( \frac{a_s \hbar^2}{G m^3} \right)^{1/2}, \quad (\text{H9})$$

$$M_J = \frac{4}{3}\pi\rho \left( \frac{\lambda_J}{2} \right)^3 = \frac{\pi}{6}\rho \left( \frac{4\pi^2 a_s \hbar^2}{G m^3} \right)^{3/2}. \quad (\text{H10})$$

The Jeans surface density is

$$\Sigma_J = \rho \frac{\lambda_J}{2} = \pi\rho \left( \frac{a_s \hbar^2}{G m^3} \right)^{1/2}. \quad (\text{H11})$$

These equations display the same scalings as Eqs. (G17), (G18) and (44) for DM halos.

## Appendix I: The mass of the DM particle

In this Appendix, we relate the mass  $m$  of the DM particle to the cosmological constant  $\Lambda$  and to the other fundamental constants of physics.

## 1. Fermions

We have seen in Sec. II A that the minimum mass of DM halos made of fermions is given by

$$(M_h)_{\min} = 4.47 \left( \frac{\hbar^{12} \Sigma_0^3}{G^6 m^{16}} \right)^{1/5}. \quad (\text{I1})$$

It is obtained by requiring that the smallest DM halo in the Universe corresponds to the ground state of the self-gravitating Fermi gas.

On the other hand, the minimum mass of DM halos may be obtained from a quantum Jeans instability theory (see, e.g., Refs. [6, 70]) leading to the Jeans mass (H2). Let us compute the Jeans mass at the present epoch where  $\rho_{\text{m},0} = 2.66 \times 10^{-24} \text{ g cm}^{-3}$ . For a fermion mass  $m = 170 \text{ eV}/c^2$ , the Jeans mass is  $M_J = 1.10 \times 10^5 M_\odot$  [70]. It is 3 orders of magnitude smaller than the minimum mass  $(M_h)_{\min} \sim 10^8 M_\odot$  of observed DM halos. Actually, we cannot expect to have a perfect agreement between the Jeans mass computed at the present epoch and the observed minimum mass of DM halos because the linear Jeans instability took place at an earlier epoch (see Appendix I 4) and the present DM halos result from a nonlinear evolution. Therefore, we write  $(M_h)_{\min} = \chi_F M_J$ , where  $\chi_F$  is a dimensionless factor that is difficult to predict theoretically (for fermions the previous estimate gives  $\chi_F \sim 10^3$ ). Using Eq. (H2), we obtain

$$(M_h)_{\min} = 16.6 \chi_F \frac{\hbar^3 \rho_{\text{m},0}^{1/2}}{G^{3/2} m^4}. \quad (\text{I2})$$

Comparing (I1) and (I2) we get

$$m = 5.16 \chi_F^{5/4} \frac{\hbar^{3/4} \rho_{\text{m},0}^{5/8}}{\Sigma_0^{3/4} G^{3/8}}. \quad (\text{I3})$$

This relation gives the surface density  $\Sigma_0$  of the smallest DM halo if we know the fermion mass  $m$ . Inversely, since  $\Sigma_0$  appears to have a universal value (see Eq. (1)), we can use Eq. (I3) to obtain the fermion mass  $m$ . More precisely, since  $\rho_{\text{m},0}$  and  $\Sigma_0$  can be expressed in terms of the cosmological constant  $\Lambda$  by Eqs. (140) and (141), we find that the mass of the fermionic particle is given by

$$m = 7.62 \chi_F^{5/4} \left( \frac{\Lambda \hbar^3}{G c^3} \right)^{1/4}. \quad (\text{I4})$$

It is equal to the mass scale  $m_\Lambda^* = 5.04 \times 10^{-3} \text{ eV}/c^2$  given by Eq. (160) multiplied by a large numerical factor of order  $4 \times 10^4$  (for  $\chi_F \sim 10^3$ ). This gives  $m \sim 200 \text{ eV}/c^2$  which is the correct order of magnitude of the fermion mass usually advocated in DM models (see Appendix D of [14]). We note that, up to the dimensionless factor  $\chi_F$ , this mass scale has been predicted in terms of the fundamental constants independently from the observations.

*Remark:* We can obtain these results (without the prefactor) directly from the Jeans scales of Appendix H 1. From Eq. (H4), we have

$$\Sigma \sim \frac{\hbar \rho^{5/6}}{m^{4/3} G^{1/2}} \quad \text{i.e.} \quad m \sim \frac{\hbar^{3/4} \rho^{5/8}}{\Sigma^{3/4} G^{3/8}}. \quad (\text{I5})$$

If we take  $\rho \sim \rho_{\text{m},0} \sim \Lambda/G$  and  $\Sigma \sim c\sqrt{\Lambda}/G$  (see Eqs. (140) and (141)), we get

$$m \sim \left( \frac{\Lambda \hbar^3}{G c^3} \right)^{1/4} \sim m_\Lambda^*. \quad (\text{I6})$$

Inversely, if we assume that  $\rho \sim \rho_{\text{m},0} \sim \Lambda/G$  and  $m \sim m_\Lambda^*$  we find that  $\Sigma \sim c\sqrt{\Lambda}/G$ . We also note that  $\lambda \sim \Sigma/\rho \sim c/\sqrt{\Lambda}$  and  $M \sim \rho \lambda^3 \sim c^3/G\sqrt{\Lambda}$  are the cosmological scales corresponding to the size and mass of the Universe [60].

## 2. Noninteracting bosons

We have seen in Sec. II B that the minimum mass of DM halos made of noninteracting bosons is given by

$$(M_h)_{\text{min}} = 1.61 \left( \frac{\hbar^4 \Sigma_0}{G^2 m^4} \right)^{1/3}. \quad (\text{I7})$$

On the other hand, the quantum Jeans instability theory [6, 70] leads to the Jeans mass (H6). For a boson mass  $m = 2.92 \times 10^{-22} \text{ eV}/c^2$ , the Jeans mass computed at the present epoch where  $\rho_{\text{m},0} = 2.66 \times 10^{-24} \text{ g m}^{-3}$  is  $M_J = 3.07 \times 10^6 M_\odot$  [70]. It is 1 order of magnitude smaller than the minimum mass  $(M_h)_{\text{min}} \sim 10^8 M_\odot$  of observed DM halos. Writing  $(M_h)_{\text{min}} = \chi_B M_J$  with  $\chi_B \sim 10$ , we obtain

$$(M_h)_{\text{min}} = 6.88 \chi_B \frac{\hbar^{3/2} \rho_{\text{m},0}^{1/4}}{G^{3/4} m^{3/2}}. \quad (\text{I8})$$

Comparing Eqs. (I7) and (I8) we get

$$m = 6089 \chi_B^6 \frac{\hbar \rho_{\text{m},0}^{3/2}}{\Sigma_0^2 G^{1/2}}. \quad (\text{I9})$$

Using Eqs. (140) and (141), we find that the mass of the bosonic particle (in the noninteracting case) is given by

$$m = 33748 \chi_B^6 \frac{\hbar \sqrt{\Lambda}}{c^2}. \quad (\text{I10})$$

It is equal to the mass scale  $m_\Lambda = 2.08 \times 10^{-33} \text{ eV}/c^2$  given by Eq. (143) multiplied by a huge numerical factor of order  $3 \times 10^{10}$  (for  $\chi_B \sim 10$ ). This gives  $m \sim 10^{-22} \text{ eV}/c^2$  which is the correct order of magnitude of the mass of ultralight axions usually advocated in DM models (see Appendix D of [14]).

*Remark:* We can obtain these results (without the prefactor) directly from the Jeans scales of Appendix H 2. From Eq. (H8), we have

$$\Sigma \sim \left( \frac{\hbar^2 \rho^3}{G m^2} \right)^{1/4} \quad \text{i.e.} \quad m \sim \left( \frac{\hbar^2 \rho^3}{G \Sigma^4} \right)^{1/2}. \quad (\text{I11})$$

If we take  $\rho \sim \rho_{\text{m},0} \sim \Lambda/G$  and  $\Sigma \sim c\sqrt{\Lambda}/G$  (see Eqs. (140) and (141)), we get

$$m \sim \frac{\hbar \sqrt{\Lambda}}{c^2} \sim m_\Lambda. \quad (\text{I12})$$

Inversely, if we assume that  $\rho \sim \rho_{\text{m},0} \sim \Lambda/G$  and  $m \sim m_\Lambda$  we find that  $\Sigma \sim c\sqrt{\Lambda}/G$ .

## 3. Self-interacting bosons in the TF limit

We have seen in Sec. II C that the minimum mass of DM halos made of self-interacting bosons in the TF limit is given by

$$(M_h)_{\text{min}} = 13.0 \frac{a_s \hbar^2 \Sigma_0}{G m^3}. \quad (\text{I13})$$

On the other hand, the quantum Jeans instability theory [6, 70] leads to the Jeans mass (H10). For a ratio  $a_s/m^3 = 3.28 \times 10^3 \text{ fm (eV}/c^2)^{-3}$ , the Jeans mass computed at the present epoch where  $\rho_{\text{m},0} = 2.66 \times 10^{-24} \text{ g m}^{-3}$  is  $M_J = 165 M_\odot$  [70]. It is 6 order of magnitude smaller than the minimum mass  $(M_h)_{\text{min}} \sim 10^8 M_\odot$  of observed DM halos. Writing  $(M_h)_{\text{min}} = \chi_{\text{TF}} M_J$  with  $\chi_{\text{TF}} \sim 10^6$ , we obtain

$$(M_h)_{\text{min}} = 130 \chi_{\text{TF}} \rho_{\text{m},0} \left( \frac{a_s \hbar^2}{G m^3} \right)^{3/2}. \quad (\text{I14})$$

Comparing (I13) and (I14) we get

$$\frac{a_s}{m^3} = \frac{0.01}{\chi_{\text{TF}}^2} \frac{G \Sigma_0^2}{\hbar^2 \rho_{\text{m},0}^2}. \quad (\text{I15})$$

Using Eqs. (140) and (141), we find that the ratio  $a_s/m^3$  is given by

$$\frac{a_s}{m^3} = \frac{0.0135}{\chi_{\text{TF}}^2} \frac{G c^2}{\Lambda \hbar^2}. \quad (\text{I16})$$

It is equal to the scale  $r_\Lambda/m_\Lambda^3 = 2Gc^2/\Lambda \hbar^2 = 6.11 \times 10^{17} \text{ fm (eV}/c^2)^{-3}$  given by Eq. (151) multiplied by a very small numerical factor of order  $10^{-14}$  (for  $\chi_{\text{TF}} \sim 10^6$ ). This gives  $a_s/m^3 \sim 10^3 \text{ fm (eV}/c^2)^{-3}$  which is the correct order of magnitude of the parameter  $a_s/m^3$  of self-interacting bosons usually advocated in DM models (see Appendix D of [14]).

*Remark:* We can obtain these results (without the prefactor) directly from the Jeans scales of Appendix H 3. From Eq. (H11), we have

$$\Sigma \sim \rho \left( \frac{a_s \hbar^2}{G m^3} \right)^{1/2} \quad \text{i.e.} \quad \frac{a_s}{m^3} \sim \frac{G \Sigma^2}{\hbar^2 \rho^2}. \quad (\text{I17})$$

If we take  $\rho \sim \rho_{m,0} \sim \Lambda/G$  and  $\Sigma \sim c\sqrt{\Lambda}/G$  (see Eqs. (140) and (141)), we get

$$\frac{a_s}{m^3} \sim \frac{Gc^2}{\Lambda\hbar^2} \sim \frac{r_\Lambda}{m_\Lambda^3}. \quad (\text{I18})$$

Inversely, if we assume that  $\rho \sim \rho_{m,0} \sim \Lambda/G$  and  $a_s/m^3 \sim r_\Lambda/m_\Lambda^3$  we find that  $\Sigma \sim c\sqrt{\Lambda}/G$ .

#### 4. Comment

We can make the following observations. For fermions, we note that  $\chi_F \rho_{m,0}^{1/2} = (\chi_F^2 \rho_{m,0})^{1/2} = (10^6 \rho_{m,0})^{1/2}$ . For noninteracting bosons, we note that  $\chi_B \rho_{m,0}^{1/4} = (\chi_B^4 \rho_{m,0})^{1/4} = (10^4 \rho_{m,0})^{1/4}$ . For self-interacting bosons

in the TF limit, we note that  $\chi_{\text{TF}} \rho_{m,0} = 10^6 \rho_{m,0}$ . These relations suggest that  $(M_h)_{\text{min}}$  is not equal to the present Jeans length but rather to the Jeans length at the epoch where the density of the Universe is  $\sim 10^5 \rho_{m,0}$ . Indeed, if we calculate the Jeans mass at the epoch where the density of the Universe is  $10^5 \rho_{m,0}$ , we find in the three cases considered above that  $M_J \sim (M_h)_{\text{min}}$ . Using  $\rho_m = \rho_{m,0}/a^3$  and  $z+1 = 1/a$  (redshift), this epoch corresponds to

$$\rho_m = 2.66 \times 10^{-19} \text{ g m}^{-3}, \quad a = 0.0215, \quad z = 45.5. \quad (\text{I19})$$

It is intermediate between the epoch of radiation-matter equality ( $\rho_{\text{eq}} = 8.77 \times 10^{-14} \text{ g m}^{-3}$ ,  $a_{\text{eq}} = 2.95 \times 10^{-4}$ ,  $z_{\text{eq}} = 3389$ ) and the present epoch ( $\rho_{m,0} = 2.66 \times 10^{-24} \text{ g m}^{-3}$ ,  $a_0 = 1$ ,  $z_0 = 0$ ).

- 
- [1] Planck Collaboration, *Astron. Astrophys.* **571**, 66 (2014)
  - [2] Planck Collaboration, *Astron. Astrophys.* **594**, A13 (2016)
  - [3] J.F. Navarro, C.S. Frenk, S.D.M. White, *Astrophys. J.* **462**, 563 (1996)
  - [4] A. Burkert, *Astrophys. J.* **447**, L25 (1995)
  - [5] G. Kauffmann, S.D.M. White, B. Guiderdoni, *Mon. Not. R. astr. Soc.* **264**, 201 (1993); A. Klypin, A.V. Kravtsov, O. Valenzuela, *Astrophys. J.* **522**, 82 (1999); M. Kamionkowski, A.R. Liddle, *Phys. Rev. Lett.* **84**, 4525 (2000)
  - [6] P.H. Chavanis, *Phys. Rev. D* **84**, 043531 (2011)
  - [7] P.H. Chavanis, arXiv:1810.08948
  - [8] A. Suárez, V.H. Robles, T. Matos, *Astrophys. Space Sci. Proc.* **38**, 107 (2014)
  - [9] T. Rindler-Daller, P.R. Shapiro, *Astrophys. Space Sci. Proc.* **38**, 163 (2014)
  - [10] P.H. Chavanis, *Self-gravitating Bose-Einstein condensates*, in *Quantum Aspects of Black Holes*, edited by X. Calmet (Springer, 2015)
  - [11] D. Marsh, *Phys. Rep.* **643**, 1 (2016)
  - [12] J.W. Lee, EPJ Web of Conferences **168**, 06005 (2018)
  - [13] E. Braaten, H. Zhang, arXiv:1810.11473
  - [14] A. Suárez, P.H. Chavanis, *Phys. Rev. D* **95**, 063515 (2017)
  - [15] D. Lynden-Bell, *Mon. Not. R. Astron. Soc.* **136**, 101 (1967)
  - [16] E. Seidel, W.M. Suen, *Phys. Rev. Lett.* **72**, 2516 (1994)
  - [17] F.S. Guzmán, L.A. Ureña-López, *Phys. Rev. D* **69**, 124033 (2004)
  - [18] F.S. Guzmán, L.A. Ureña-López, *Astrophys. J.* **645**, 814 (2006)
  - [19] J.R. Oppenheimer, G.M. Volkoff, *Phys. Rev.* **55**, 374 (1939)
  - [20] D.J. Kaup, *Phys. Rev.* **172**, 1331 (1968)
  - [21] R. Ruffini, S. Bonazzola, *Phys. Rev.* **187**, 1767 (1969)
  - [22] M. Colpi, S.L. Shapiro, I. Wasserman, *Phys. Rev. Lett.* **57**, 2485 (1986)
  - [23] I.I. Tkachev, *Sov. Astron. Lett.* **12**, 305 (1986)
  - [24] P.H. Chavanis, T. Harko, *Phys. Rev. D* **86**, 064011 (2012)
  - [25] H.Y. Schive, T. Chiueh, T. Broadhurst, *Nature Physics* **10**, 496 (2014)
  - [26] H.Y. Schive *et al.*, *Phys. Rev. Lett.* **113**, 261302 (2014)
  - [27] L. Hui, J. Ostriker, S. Tremaine, E. Witten, *Phys. Rev. D* **95**, 043541 (2017)
  - [28] B. Bar-Or, J.B. Fouvry, S. Tremaine, *Astrophys. J.* **871**, 28 (2019)
  - [29] J. Binney, S. Tremaine, *Galactic Dynamics* (Princeton, NJ: Princeton University Press, 1987)
  - [30] J. Kormendy, K.C. Freeman, in S.D. Ryder, D.J. Pisano, M.A. Walker, K.C. Freeman, eds., *Proc. IAU Symp. 220, Dark Matter in Galaxies*. Astron. Soc. Pac., San Francisco, p. 377 (2004)
  - [31] M. Spano, M. Marcelin, P. Amram, C. Carignan, B. Epinat, O. Hernandez, *Mon. Not. R. Astron. Soc.* **383**, 297 (2008)
  - [32] F. Donato *et al.*, *Mon. Not. R. Astron. Soc.* **397**, 1169 (2009)
  - [33] P.H. Chavanis, *Phys. Rev. E* **65**, 056123 (2002)
  - [34] P. Mocz *et al.*, *Mon. Not. R. Astron. Soc.* **471**, 4559 (2017)
  - [35] S. Chandrasekhar, *An Introduction to the Theory of Stellar Structure* (Dover, 1942)
  - [36] E. Madelung, *Zeit. F. Phys.* **40**, 322 (1927)
  - [37] M. Membrado, A.F. Pacheco, J. Sanudo, *Phys. Rev. A* **39**, 4207 (1989)
  - [38] P.H. Chavanis, L. Delfini, *Phys. Rev. D* **84**, 043532 (2011)
  - [39] D. Marsh, A.R. Pop, *Monthly Not. Roy. Astron.* **451**, 2479 (2015)
  - [40] M. Membrado, J. Abad, A.F. Pacheco, J. Sañudo, *Phys. Rev. D* **40**, 2736 (1989)
  - [41] J.W. Lee, I. Koh, *Phys. Rev. D* **53**, 2236 (1996)
  - [42] J. Goodman, *New Astronomy* **5**, 103 (2000)
  - [43] A. Arbey, J. Lesgourgues, P. Salati, *Phys. Rev. D* **68**, 023511 (2003)
  - [44] C.G. Böhm, T. Harko, *J. Cosmol. Astropart. Phys.* **06**, 025 (2007)
  - [45] S.W. Randall, M. Markevitch, D. Clowe, A.H. Gonzalez, M. Bradac, *Astrophys. J.* **679**, 1173 (2008)
  - [46] E. Braaten, A. Mohapatra, H. Zhang, *Phys. Rev. Lett.* **117**, 121801 (2016)



- [47] E. Cotner, Phys. Rev. D **94**, 063503 (2016)
- [48] P.H. Chavanis, Phys. Rev. D **94**, 083007 (2016)
- [49] J. Eby *et al.*, JHEP **12**, 066 (2016)
- [50] D.G. Levkov, A.G. Panin, I.I. Tkachev, Phys. Rev. Lett. **118**, 011301 (2017)
- [51] T. Helfer *et al.*, JCAP **03**, 055 (2017)
- [52] P.H. Chavanis, Phys. Rev. D **98**, 023009 (2018)
- [53] L. Visinelli, S. Baum, J. Redondo, K. Freese, F. Wilczek, Phys. Lett. B **777**, 64 (2018)
- [54] F. Michel, I.G. Moss, Phys. Lett. B **785**, 9 (2018)
- [55] P.H. Chavanis, Eur. Phys. J. Plus **132**, 248 (2017)
- [56] P.H. Chavanis, Phys. Dark Univ. **22**, 80 (2018)
- [57] P.H. Chavanis, Int. J. Mod. Phys. B **20**, 3113 (2006)
- [58] P.H. Chavanis, Eur. Phys. J. Plus **130**, 130 (2015)
- [59] P.H. Chavanis, Phys. Lett. B **758**, 59 (2016)
- [60] P.H. Chavanis, Phys. Dark Univ. **24**, 100271 (2019)
- [61] A. Arvanitaki, S. Dimopoulos, S. Dubovsky, N. Kaloper, J. March-Russell, Phys. Rev. D **81**, 123530 (2010)
- [62] A.S. Goldhaber, M.M. Nieto, Rev. Mod. Phys. **82**, 939 (2010)
- [63] P.H. Chavanis, M. Lemou, F. Méhats, Phys. Rev. D **92**, 123527 (2015)
- [64] R. Ruffini, C.R. Argüelles, J.A. Rueda, Mon. Not. R. Astron. Soc. **451**, 622 (2015)
- [65] P.H. Chavanis, preprint
- [66] R. Emden, *Gaskugeln* (Teubner Verlag, Leipzig, 1907)
- [67] A. Schuster, Brit. Assoc. Rept., P. 427 (1883)
- [68] H.C. Plummer, Mon. Not. R. Astron. Soc. **71**, 460 (1911)
- [69] P. Ledoux, C.L. Pekeris, Astrophys. J. **94**, 124 (1941)
- [70] A. Suárez, P.H. Chavanis, Phys. Rev. D **98**, 083529 (2018)